

STRING KERNEL REPRESENTATIONS IN ELASTOSTATICS

Jeremy G. Hoskins¹, Alan E. Lindsay², and Manas Rachh³

ABSTRACT. In this paper we present a new boundary integral equation formulation for the solution of the elastostatic traction boundary value problem in two and three dimensions. The approach relies on the introduction of new layer potentials, called *string kernels*, which are based on modifications of the Boussinesq-Cerruti family of half-space solutions. We prove that the resulting integral equations are second-kind integral equations, and show that they are well-behaved in the incompressible limit. We illustrate the performance of the method with several numerical examples.

1. INTRODUCTION

In this paper we consider the problem of linear elastostatics with traction boundary conditions in two and three dimensions, modeled by the boundary value problem

$$(1) \quad L[u](\mathbf{x}) := (\lambda + \mu)\nabla(\nabla \cdot u(\mathbf{x})) + \mu\Delta u(\mathbf{x}) = 0, \quad \mathbf{x} \in \Omega,$$

$$(2) \quad \hat{\mathbf{n}}(\mathbf{x}) \cdot \sigma[u](\mathbf{x}) = f(\mathbf{x}), \quad \mathbf{x} \in \partial\Omega,$$

where λ and μ are the Lamé parameters, u is an unknown displacement field, $\hat{\mathbf{n}}(\mathbf{x})$ denotes the outward normal, and the stress σ is defined by

$$\sigma_{ij}[u] = \lambda\delta_{ij}\frac{\partial u_k}{\partial x_k} + \mu\left(\frac{\partial u_j}{\partial x_i} + \frac{\partial u_i}{\partial x_j}\right),$$

where δ_{ij} is the Kronecker delta function and we employ the standard Einstein summation convention. In what follows we will assume that $\partial\Omega$ is infinitely differentiable and compact, though Ω can be either bounded or unbounded. It is well-known (see [40] for example) that for the interior problem the above boundary value problem has a finite-dimensional nullspace corresponding to rigid motions. Existence requires the applied traction to have zero net force and zero net torque. On unbounded domains, one must also impose suitable decay conditions at infinity.

There is a large literature on solving the traction boundary value problem using finite difference and finite element methods, see [9, 74, 2, 23, 15, 26, 27], for example. Direct discretization of the PDE, however, carries several well-known difficulties, particularly for complex domains requiring adaptivity, since the condition number of the resulting sparse linear systems grows as h^{-2} under mesh refinement. Additionally, exterior and unbounded problems require artificial domain truncation. These issues are compounded as the

¹Department of Statistics, University of Chicago, USA and NSF-Simons National Institute for Theory and Mathematics in Biology, Chicago, IL. Email: jeremyhoskins@uchicago.edu

²University of Notre Dame, Notre Dame, IN, 46556, USA. Email: a.lindsay@nd.edu

³Department of Mathematics, Indian Institute of Technology Bombay, Powai, Mumbai - 400076
Email: mrachh@iitb.ac.in

material approaches the incompressible limit $\lambda \rightarrow \infty$: standard conforming displacement-based finite element methods can exhibit volumetric locking, and the resulting linear systems become increasingly ill-conditioned, with error and conditioning bounds that are not uniform in λ [7, 14, 10]. Recovering uniform behavior requires non-conforming, mixed, or stabilized formulations that satisfy an inf-sup (LBB) condition, as in the incompressible-Stokes case to which elastostatics formally reduces in this limit.

Boundary integral equation (BIE) methods, by contrast, discretize only the boundary of the domain. This leads to a reduction in the dimension of the problem, straightforward treatment of exterior problems and unbounded domains, and the treatment of complex geometries without volumetric meshing. Moreover, for many PDEs and for suitably chosen ansatzes, this reduction to a BIE produces second-kind integral equations whose condition number remains bounded independent of discretization size [47]. A further practical advantage of the BIE framework is that derived quantities such as stress are computed by applying the relevant differential operator to the kernel, and retain the full convergence rate of the boundary discretization at any point bounded away from $\partial\Omega$. With appropriate near-singular quadrature or adaptive integration, these quantities can frequently be accurately computed up to and on $\partial\Omega$ itself.

In two dimensions, the standard integral-equation-based approach for solving the traction boundary value problem is to use the Sherman-Lauricella representation [50, 66]. This approach has subsequently been extended to traction boundary value problems on multiply connected domains in [34, 37]. For a detailed discussion and related problems in elasticity, see [60, 55, 58, 41, 42]. However, the Sherman-Lauricella representation does not extend naturally to three dimensions, as the method relies on enforcing indefinite integrals of the surface traction, rather than the value of the surface traction itself.

Another class of integral-equation-based approaches involves *direct representations*, which are based on the Somigliana identity (the elastostatic analog of Green's identity). This approach tends to result in integral equations involving singular or hypersingular integral operators in two and three dimensions [11, 40, 70]. Alternatively, indirect representations seek to represent the solution to the PDE as integrals of unknown densities on the boundary $\partial\Omega$ against kernels constructed from linear combinations of the free-space elastostatics Green's function and its derivatives. This choice also results in a singular integral operator upon imposing the boundary conditions [70, 38].

In both the typical indirect and direct representations, the resulting integral operator is Fredholm of index zero but is not a compact perturbation of the identity, in contrast to the Laplace Neumann problem, where the single-layer ansatz produces the classical second-kind equation $\frac{1}{2}I + K^*$. Consequently, the standard machinery for second-kind equations is not directly applicable. Nevertheless, a variety of quadrature methods have

been developed to address singular and hypersingular integral operators, see [30, 1, 65, 43, 72], for example.

Our approach represents the displacement field using a layer potential on $\partial\Omega$ whose kernel is built from modifications of the Boussinesq-Cerruti family of half-space fundamental solutions [12, 19, 52], i.e., the Green's functions for a point load acting in a half-space with zero traction boundary conditions. Since the Boussinesq-Cerruti solutions already satisfy the zero-traction condition on a flat half-space boundary, they are an appealing candidate kernel for traction boundary value problems on general domains. They do, however, carry a non-local singularity: in addition to the expected singularity at the source, each kernel is singular along a half-line emanating from the source in the direction complementary to the half-space. This geometric obstruction rules out their direct use as layer-potential kernels on non-convex domains and for exterior problems, where such half-lines generically intersect the solution domain.

A key observation is that each Boussinesq-Cerruti kernel admits a representation as a line integral of certain derivatives of the free-space elastostatic fundamental solution along this half-line. Truncating the integration to a finite segment produces what we call a *string kernel*: near the source the singularity structure inherited from the free-space kernel is preserved, while the extended singularity is now confined to a bounded segment which, by appropriate choice of string orientation and length, can be made to lie entirely outside $\bar{\Omega}$ regardless of the domain geometry. The full Boussinesq-Cerruti representation is recovered as the string length tends to infinity. Using a string kernel as the integrand of a layer potential with a density supported on $\partial\Omega$ gives a second-kind boundary integral equation that is well-behaved in the limit $\lambda \rightarrow \infty$, μ fixed.

A distinct, though conceptually related, class of methods is the method of fundamental solutions (MFS) [25, 18, 20, 45, 48], in which finite collections of point sources, called *image charges*, are placed outside of the domain. The strengths of the image charges are inferred from symmetry, precomputed by a local auxiliary solve, or included as additional unknowns in the global linear system. As such, though effective in practice, the result does not typically correspond to a discretization of a second-kind integral equation, and hence comes with fewer analytic guarantees on conditioning and convergence. In the context of MFS, string kernel representations use a continuum of image charges with known relative strengths (per string) confined only to line segments.

The contributions of this paper are as follows. We introduce a family of *string kernel* layer-potential representations for the traction boundary value problem of linear elastostatics in two and three dimensions, derived by truncating the line-integral representation of the Boussinesq-Cerruti half-space fundamental solutions. We prove that, for smooth $\partial\Omega$ and an appropriate choice of string orientation and length, the resulting boundary integral operator is a compact perturbation of a multiple of the identity, and hence

that the associated boundary integral equation is of second kind. Naturally, the condition number of the representations deteriorates when the string length goes to zero. In two dimensions we show that the strings can be *bent*, allowing for longer strings and almost entirely avoiding this issue. Furthermore, we show that the condition number is independent of λ . Indeed, the integral equation itself is independent of λ . In three dimensions, we present numerical experiments showing the behavior of the conditioning of our representation as the string length goes to zero. Additionally, under certain assumptions, we show that the condition number of our integral equation is bounded as $\lambda \rightarrow \infty$ with μ held fixed, and in this limit reduces to a compact perturbation of a standard second-kind integral equation for the Stokes traction problem.

The remainder of the paper is organized as follows. In Section 2 we review the Boussinesq solutions and the properties of layer potentials generated using them. Next, in Section 3 we introduce string kernel representations and use them to derive our second-kind integral equation for elastostatics. In Section 4 we describe numerical considerations required when using string kernels, including stable evaluation and choice of string length. Following this, in Section 5, we illustrate the application of our approach to 2D and 3D examples.

2. BOUSSINESQ-CERRUTI SOLUTIONS IN TWO AND THREE DIMENSIONS

2.1. Notation, definitions, and basic properties. Our boundary integral representations for solving (1-2) are based on suitable modifications of the fundamental solution of half-space elastostatics problems. In particular, we take as our starting point the Boussinesq-Cerruti solutions [12] in two and three dimensions for point loads on a semi-infinite isotropic elastic medium. We refer the reader to [49], for example, for further discussion and derivations.

In two dimensions, given a source $\mathbf{y} = (y_1, y_2)^T$, a target $\mathbf{x} = (x_1, x_2)^T$, and a unit direction vector $\hat{\mathbf{v}} = (v_1, v_2)^T$, we define the matrix-valued function $G^{B,2}$ by

$$G^{B,2}(\mathbf{x}, \mathbf{y}; \hat{\mathbf{v}}) = 2G^{S,2}(\mathbf{x}, \mathbf{y}) + \frac{1}{2\pi\mu} \frac{1-\alpha}{\alpha} \arg(\hat{\mathbf{v}}^\perp \cdot \mathbf{r}, -\hat{\mathbf{v}} \cdot \mathbf{r}) \begin{pmatrix} 0 & 1 \\ -1 & 0 \end{pmatrix}$$

where $\alpha = (\lambda + \mu)/(\lambda + 2\mu)$, $\mathbf{r} = \mathbf{x} - \mathbf{y}$, $r = |\mathbf{r}|$, $\hat{\mathbf{v}}^\perp = (v_2, -v_1)$, $\arg(u, v)$ denotes the argument of $v + iu$ with branch cut along the negative real axis, and $G^{S,2}$ is the 2D Stokeslet [46, 61]

$$(3) \quad G^{S,2}(\mathbf{x}, \mathbf{y}) = \frac{1}{2\pi\mu} \left[-\log(r) \mathbf{I}_2 + \frac{\mathbf{r}\mathbf{r}^T}{r^2} \right].$$

Here \mathbf{I}_d denotes the $d \times d$ identity matrix. Let $G^{D,2}(\mathbf{x}, \mathbf{y}; \hat{\mathbf{v}}) := G^{B,2}(\mathbf{x}, \mathbf{y}; \hat{\mathbf{v}}) - 2G^{S,2}(\mathbf{x}, \mathbf{y})$.

A straightforward calculation shows that

$$L[G^{B,2}(\cdot, \mathbf{y}; \hat{\mathbf{v}})](\mathbf{x}) = 0,$$

for all $\mathbf{x} \in \mathbb{R}^2 \setminus \mathcal{L}_{\mathbf{y}, \hat{\mathbf{v}}}$, where $\mathcal{L}_{\mathbf{y}, \hat{\mathbf{v}}} = \{\mathbf{x} \mid \mathbf{x} = \mathbf{y} + t\hat{\mathbf{v}}, t \in \mathbb{R}^+\}$, i.e., for all \mathbf{x} which are not on the half-line starting at \mathbf{y} and going to infinity in the $\hat{\mathbf{v}}$ direction. Moreover, again excluding this line,

$$(4) \quad \sigma[G^{B,2}(\cdot, \mathbf{y}; \hat{\mathbf{v}})]_{ijk}(\mathbf{x}) = 2\sigma[G^{S,2}(\cdot, \mathbf{y})]_{ijk}(\mathbf{x}) = -2\frac{r_i r_j r_k}{\pi r^4},$$

and so, in particular, $\sigma[G^{D,2}] \equiv 0$.

Similarly, in three dimensions given a source $\mathbf{y} = (y_1, y_2, y_3)^T$, a target $\mathbf{x} = (x_1, x_2, x_3)^T$, and a unit direction vector $\hat{\mathbf{v}} = (v_1, v_2, v_3)^T$, we define the matrix-valued function $G^{B,3}$ by

$$G^{B,3}(\mathbf{x}, \mathbf{y}; \hat{\mathbf{v}}) = 2G^{S,3}(\mathbf{x}, \mathbf{y}) + \frac{1}{4\pi\mu} \frac{1-\alpha}{\alpha} \left[\frac{1}{R} \mathbf{I}_3 + \frac{\mathbf{r}\hat{\mathbf{v}}^T - \hat{\mathbf{v}}\mathbf{r}^T - (\mathbf{r} \cdot \hat{\mathbf{v}})\hat{\mathbf{v}}\hat{\mathbf{v}}^T}{rR} - \frac{Q_{\hat{\mathbf{v}}}\mathbf{r}\mathbf{r}^T Q_{\hat{\mathbf{v}}}}{rR^2} \right],$$

where $\mathbf{r} = \mathbf{x} - \mathbf{y}$, $r = |\mathbf{r}|$, $Q_{\hat{\mathbf{v}}} = \mathbf{I}_3 - \hat{\mathbf{v}}\hat{\mathbf{v}}^T$, $R = r - \mathbf{r} \cdot \hat{\mathbf{v}}$, where $G^{S,3}$ denotes the 3D Stokeslet [32, 16, 68]

$$(5) \quad G^{S,3}(\mathbf{x}, \mathbf{y}) = \frac{1}{4\pi\mu} \left[\frac{\mathbf{I}_3}{r} + \frac{\mathbf{r}\mathbf{r}^T}{r^3} \right].$$

Let $G^{D,3}(\mathbf{x}, \mathbf{y}; \hat{\mathbf{v}}) := G^{B,3}(\mathbf{x}, \mathbf{y}; \hat{\mathbf{v}}) - 2G^{S,3}(\mathbf{x}, \mathbf{y})$.

Again, a straightforward but tedious calculation shows that

$$L[G^{B,3}(\cdot, \mathbf{y}; \hat{\mathbf{v}})](\mathbf{x}) = 0,$$

at all points \mathbf{x} which are not on the half-line $\mathcal{L}_{\mathbf{y}, \hat{\mathbf{v}}}$, and

$$\begin{aligned} \sigma[G^{B,3}(\cdot, \mathbf{y}; \hat{\mathbf{v}})]_{ijk}(\mathbf{x}) = & -\frac{6\mathbf{r}_i \mathbf{r}_j \mathbf{r}_k}{4\pi r^5} + \frac{1}{4\pi} \frac{1-\alpha}{\alpha} \left\{ \left(\frac{4}{R} + \frac{2}{r} \right) \frac{(Q_{\hat{\mathbf{v}}}\mathbf{r})_i (Q_{\hat{\mathbf{v}}}\mathbf{r})_j \mathbf{r}_k}{r^2 R^2} \right. \\ & - 2 \frac{(Q_{\hat{\mathbf{v}}})_{i,j} \mathbf{r}_k}{r} \left(\frac{1}{R^2} - \frac{1}{r^2} \right) - 4 \frac{(Q_{\hat{\mathbf{v}}}\mathbf{r})_i (Q_{\hat{\mathbf{v}}}\mathbf{r})_j \hat{\mathbf{v}}_k}{r R^3} \\ & \left. + \frac{2(Q_{\hat{\mathbf{v}}})_{i,j} \hat{\mathbf{v}}_k}{R^2} - 2 \frac{(Q_{\hat{\mathbf{v}}})_{i,k} (Q_{\hat{\mathbf{v}}}\mathbf{r})_j + (Q_{\hat{\mathbf{v}}})_{j,k} (Q_{\hat{\mathbf{v}}}\mathbf{r})_i}{r R^2} \right\}. \end{aligned}$$

2.2. Boussinesq-Cerruti layer potentials. In this section we review results on limits of the normal stress of layer potentials constructed from Stokeslets, and prove analogous results for the difference integral kernels $G^{D,2}$ and $G^{D,3}$. The following standard theorem characterizes the normal stress of Stokeslet layer potentials.

Theorem 2.1. *Let Ω be a simply connected domain in \mathbb{R}^d , $d = 2, 3$ with smooth boundary $\partial\Omega$. For $\rho \in L^2(\partial\Omega; \mathbb{R}^d)$,*

$$\lim_{\delta \rightarrow 0^+} \hat{\mathbf{n}}_i(\mathbf{x}) \sigma \left[\int G^{S,d}(\cdot, \mathbf{y}) \rho(\mathbf{y}) \, dS(\mathbf{y}) \right]_{ijk}(\mathbf{x} - \delta \hat{\mathbf{n}})$$

$$= \frac{1}{2}\rho_j(\mathbf{x}) + \int \hat{\mathbf{n}}_i(\mathbf{x})\sigma[G^{S,d}(\cdot, \mathbf{y})]_{ijk}(\mathbf{x})\rho_k(\mathbf{y})\,dS(\mathbf{y}),$$

in an L^2 sense. Moreover, the integral operator on the right-hand side is compact from $L^2(\partial\Omega; \mathbb{R}^d)$ to itself.

Proof. The proof follows from standard arguments. For continuous densities, ρ , the corresponding limits can be found in [40], for example. From these, the L^2 statement can be obtained using a similar argument as in [44, 47]. \square

We now turn to the difference kernels $G^{D,2}, G^{D,3}$ with the specific choice $\hat{\mathbf{v}}(\mathbf{y}) = \hat{\mathbf{n}}(\mathbf{y})$, the outward facing normal. These functions have discontinuities or singularities on the half-line $\mathcal{L}_{\mathbf{y}, \hat{\mathbf{v}}}$ and so, where these half-lines intersect the boundary, the stress will not be well-defined. This issue is a *nonlocal* phenomenon in so far as the singularities arising near a point $\mathbf{x} \in \partial\Omega$ are due to the density at points $\mathbf{y} \in \partial\Omega$ which lie outside of an open neighborhood of \mathbf{x} . In light of this, we analyze the kernels after multiplying by sufficiently narrow bump functions.

To that end, in the following we let $\chi : \mathbb{R} \rightarrow \mathbb{R}$ be a smooth function which is identically 1 for $|x| \leq 1/2$, and identically zero for $|x| \geq 1$. For any $r > 0$ set $\chi_r(x) = \chi(x/r)$. For a simply connected domain Ω in \mathbb{R}^2 or \mathbb{R}^3 with smooth boundary $\partial\Omega$ set

$$\beta(\Omega) = \sup\{t \in \mathbb{R}^+ \mid \mathbf{x} + s\hat{\mathbf{n}}(\mathbf{x}) \notin \Omega, \text{ for all } s \in (0, t), \mathbf{x} \in \partial\Omega\},$$

and $\beta'(\Omega) = \min\{1, \beta(\Omega)/2\}$. For ease of exposition when there is no risk of confusion we will write β' in place of $\beta'(\Omega)$.

Theorem 2.2. *Let Ω be a simply connected domain in \mathbb{R}^d , $d = 2, 3$ with smooth boundary $\partial\Omega$, and β' be defined as above. For $\rho \in L^2(\partial\Omega; \mathbb{R}^d)$,*

$$\begin{aligned} & \lim_{\delta \rightarrow 0^+} \hat{\mathbf{n}}_i(\mathbf{x})\sigma \left[\int G^{D,d}(\cdot, \mathbf{y}; \hat{\mathbf{n}}(\mathbf{y}))\chi_{\beta'}(|\cdot - \mathbf{y}|)\rho_k(\mathbf{y})\,dS(\mathbf{y}) \right]_{ijk}(\mathbf{x} - \delta\hat{\mathbf{n}}) \\ &= \int \hat{\mathbf{n}}_i(\mathbf{x})\sigma[G^{D,d}(\cdot, \mathbf{y}; \hat{\mathbf{n}}(\mathbf{y}))\chi_{\beta'}(|\cdot - \mathbf{y}|)]_{ijk}(\mathbf{x})\rho_k(\mathbf{y})\,dS(\mathbf{y}), \end{aligned}$$

in an L^2 sense. Moreover, the integral operator on the right-hand side is compact from $L^2(\partial\Omega; \mathbb{R}^d)$ to itself.

Proof. We begin by observing that $G^{D,d}(\mathbf{x}, \mathbf{y}; \hat{\mathbf{n}}(\mathbf{y}))\chi_{\beta'}(|\mathbf{x} - \mathbf{y}|)$, $d = 2, 3$ is a smooth function of \mathbf{x} in the interior of Ω . Hence, for any fixed $\delta > 0$ sufficiently small, we can interchange the differentiation and integration to obtain

$$\begin{aligned} & \hat{\mathbf{n}}_i(\mathbf{x})\sigma \left[\int G^D(\cdot, \mathbf{y}; \hat{\mathbf{n}}(\mathbf{y}))\chi_{\beta'}(|\cdot - \mathbf{y}|)\rho_k(\mathbf{y})\,dS(\mathbf{y}) \right]_{ijk}(\mathbf{x} - \delta\hat{\mathbf{n}}(\mathbf{x})) \\ &= \int \hat{\mathbf{n}}_i(\mathbf{x})\sigma[G^D(\cdot, \mathbf{y}; \hat{\mathbf{n}}(\mathbf{y}))\chi_{\beta'}(|\cdot - \mathbf{y}|)]_{ijk}(\mathbf{x} - \delta\hat{\mathbf{n}}(\mathbf{x}))\rho_k(\mathbf{y})\,dS(\mathbf{y}). \end{aligned}$$

Moreover, the kernel on the right-hand side is smooth. We split it into two terms,

$$(6) \quad \begin{aligned} T_{jk}^{(1)} + T_{jk}^{(2)} &:= \hat{\mathbf{n}}_i(\mathbf{x}) \sigma[G^D(\cdot, \mathbf{y}, \hat{\mathbf{n}}(\mathbf{y}))]_{ijk}(\mathbf{x} - \delta \hat{\mathbf{n}}(\mathbf{x})) \chi_{\beta'}(|\mathbf{x} - \delta \hat{\mathbf{n}}(\mathbf{x}) - \mathbf{y}|) \\ &+ (\sigma[\chi_{\beta'}(|\cdot - \mathbf{y}|) \hat{\mathbf{n}}(\mathbf{x})]_i(\mathbf{x} - \delta \hat{\mathbf{n}}(\mathbf{x}))) G_{ijk}^D(\mathbf{x} - \delta \hat{\mathbf{n}}(\mathbf{x}), \mathbf{y}, \hat{\mathbf{n}}(\mathbf{y})), \end{aligned}$$

where in the second term, the $\hat{\mathbf{n}}(\mathbf{x})$ appearing in the argument of σ is not differentiated.

In 2D, $T^{(1)} \equiv 0$. Additionally, for $\delta > 0$ and sufficiently small, $|T_{jk}^{(2)}| \leq C \frac{|1-\alpha|}{\alpha}$, for all $j, k = 1, 2$, and all $\mathbf{x}, \mathbf{y} \in \partial\Omega$. The constant C is independent of α, μ , and δ . It follows that the integral operator with kernel $T^{(2)}$ is Hilbert-Schmidt and hence compact from $L^2(\partial\Omega; \mathbb{R}^2)$ to itself. This completes the proof.

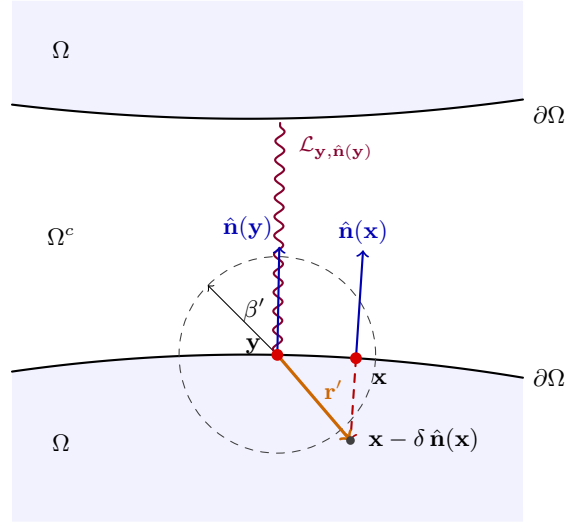


FIGURE 1. Geometry of sources, targets, and singularities.

In 3D, we first use the smoothness of kernels away from $\partial\Omega$ to show that the operators with integral kernel T are compact for $\delta > 0$ and sufficiently small, and uniformly bounded. We then show that the operator with $\delta = 0$ is the norm limit of these operators and hence is also compact. Though the proof involves fairly standard arguments, we include it here for completeness. In the following we use C to represent arbitrary constants which depend only on $\partial\Omega$.

We first bound $T^{(1)}$. For $\delta > 0$ and sufficiently small, $T_{jk}^{(1)}(\mathbf{x}, \mathbf{y}; \delta)$ is smooth and hence the resulting integral operator is compact from $L^2(\partial\Omega; \mathbb{R}^3)$ to itself. Next, if $R(\mathbf{x}, \mathbf{y}; \delta) := |\mathbf{x} - \delta \hat{\mathbf{n}}(\mathbf{x}) - \mathbf{y}| - (\mathbf{x} - \delta \hat{\mathbf{n}}(\mathbf{x}) - \mathbf{y}) \cdot \hat{\mathbf{n}}(\mathbf{y})$ for $\mathbf{x}, \mathbf{y} \in \partial\Omega$, then there exist constants $r_0, \delta_0, c > 0$, depending only on Ω , such that $|R(\mathbf{x}, \mathbf{y}; \delta)| > c|\mathbf{x} - \delta \hat{\mathbf{n}}(\mathbf{x}) - \mathbf{y}|$, whenever $|\mathbf{x} - \mathbf{y}| < r_0$ and $\delta < \delta_0$. Moreover, without loss of generality we can suppose that δ_0 is

chosen sufficiently small so that $T^{(1)}(\mathbf{x}, \mathbf{y}; \delta)$ is smooth in $\mathbf{x}, \mathbf{y} \in \partial\Omega$ for all $0 < \delta < \delta_0$. With this bound on R it follows that for all $|\mathbf{x} - \mathbf{y}| < r_0$ and $\delta < \delta_0$,

$$|T_{jk}^{(1)}(\mathbf{x}, \mathbf{y}; \delta)| \leq C \frac{|Q_{\hat{\mathbf{n}}(\mathbf{y})} \hat{\mathbf{n}}(\mathbf{x})|}{r^2}, \quad j, k = 1, 2, 3,$$

for some constant C , and with $r = |\mathbf{x} - \delta \hat{\mathbf{n}}(\mathbf{x}) - \mathbf{y}|$. If $\partial\Omega$ is twice continuously differentiable then Taylor's theorem (see [47] for example) implies that there exist constants R_0 and C such that $|Q_{\hat{\mathbf{n}}(\mathbf{y})} \hat{\mathbf{n}}(\mathbf{x})| < C|\mathbf{x} - \mathbf{y}|$ whenever $|\mathbf{x} - \mathbf{y}| < R_0$. Hence, for \mathbf{x} and \mathbf{y} sufficiently close, and δ sufficiently small,

$$|T_{jk}^{(1)}(\mathbf{x}, \mathbf{y}; \delta)| \leq C \frac{1}{|\mathbf{x} - \mathbf{y}|}.$$

Essentially identical arguments applied to $T^{(2)}$ give the bound

$$|T_{jk}^{(2)}(\mathbf{x}, \mathbf{y}; \delta)| \leq C \frac{1}{|\mathbf{x} - \mathbf{y}|}.$$

In particular, we see that the integral operators with kernels

$$T(\mathbf{x}, \mathbf{y}; \delta) = T^{(1)}(\mathbf{x}, \mathbf{y}; \delta) + T^{(2)}(\mathbf{x}, \mathbf{y}; \delta),$$

are compact, and uniformly bounded from $L^2(\partial\Omega; \mathbb{R}^3) \rightarrow L^2(\partial\Omega; \mathbb{R}^3)$ for all non-negative δ less than some positive $\hat{\delta}$, depending only on $\partial\Omega$. This follows from the fact that $T(\mathbf{x}, \mathbf{y}; \delta)$ has a weakly singular kernel bounded by $C/|\mathbf{x} - \mathbf{y}|$ with a constant C which is independent of δ , see [62] for example.

Similar arguments give that for $0 \leq \delta_1, \delta_2 < \delta_0$,

$$|T(\mathbf{x}, \mathbf{y}; \delta_1) - T(\mathbf{x}, \mathbf{y}; \delta_2)| \leq C \frac{|\delta_1 - \delta_2|}{r^2}.$$

For any $0 < \delta < \delta_0$ and any $\rho \in L^2(\partial\Omega; \mathbb{R}^3)$, and any $\epsilon > 0$, we note that

$$\begin{aligned} & \left\| \int_{\partial\Omega} T_{jk}(\mathbf{x}, \mathbf{y}; \delta) \rho_k(\mathbf{y}) \, dS(\mathbf{y}) - \int_{\partial\Omega} T_{jk}(\mathbf{x}, \mathbf{y}; 0) \rho_k(\mathbf{y}) \, dS(\mathbf{y}) \right\| \\ & \leq \left\| \int_{\partial\Omega} |T_{jk}(\mathbf{x}, \mathbf{y}; \delta) - T_{jk}(\mathbf{x}, \mathbf{y}; 0)| |\rho_k(\mathbf{y})| \, dS(\mathbf{y}) \right\| \\ & \leq \left\| \int_{\partial\Omega} \chi_\epsilon(\mathbf{x} - \mathbf{y}) |T_{jk}(\mathbf{x}, \mathbf{y}; \delta) - T_{jk}(\mathbf{x}, \mathbf{y}; 0)| |\rho_k(\mathbf{y})| \, dS(\mathbf{y}) \right\| \\ & \quad + \left\| \int_{\partial\Omega} (1 - \chi_\epsilon(\mathbf{x} - \mathbf{y})) |T_{jk}(\mathbf{x}, \mathbf{y}; \delta) - T_{jk}(\mathbf{x}, \mathbf{y}; 0)| |\rho_k(\mathbf{y})| \, dS(\mathbf{y}) \right\|. \end{aligned}$$

Here $\|\cdot\|$ denotes the norm on $L^2(\partial\Omega; \mathbb{R}^3)$. Inserting our previous bound on T into the above inequality yields

$$\begin{aligned} & \left\| \int_{\partial\Omega} T_{jk}(\mathbf{x}, \mathbf{y}; \delta) \rho_k(\mathbf{y}) \, dS(\mathbf{y}) - \int_{\partial\Omega} T_{jk}(\mathbf{x}, \mathbf{y}; 0) \rho_k(\mathbf{y}) \, dS(\mathbf{y}) \right\| \\ & \leq \left\| \int_{\partial\Omega} \chi_\epsilon(\mathbf{x} - \mathbf{y}) \frac{C}{|\mathbf{x} - \mathbf{y}|} |\rho_k(\mathbf{y})| \, dS(\mathbf{y}) \right\| + \left\| \int_{\partial\Omega} \frac{C\delta}{\epsilon^2} \|\rho(\mathbf{y})\|_{\ell^2} \, dS(\mathbf{y}) \right\|, \end{aligned}$$

where $\|\rho(\mathbf{y})\|_{\ell^2} = \sqrt{\rho_1^2(\mathbf{y}) + \rho_2^2(\mathbf{y}) + \rho_3^2(\mathbf{y})}$ is the standard Euclidean norm. The smoothness of $\partial\Omega$ implies that there is an overall constant C such that

$$\int_{\partial\Omega} \chi_\epsilon(\mathbf{x} - \mathbf{y}) \frac{1}{|\mathbf{x} - \mathbf{y}|} dS(\mathbf{y}) \leq C\epsilon,$$

for all $\mathbf{x} \in \partial\Omega$, and

$$\int_{\partial\Omega} \chi_\epsilon(\mathbf{x} - \mathbf{y}) \frac{1}{|\mathbf{x} - \mathbf{y}|} dS(\mathbf{x}) \leq C\epsilon,$$

for all $\mathbf{y} \in \partial\Omega$, and $\epsilon > 0$. It follows immediately from the Schur test [64] that

$$\left\| \int_{\partial\Omega} \chi_\epsilon(\mathbf{x} - \mathbf{y}) \frac{1}{|\mathbf{x} - \mathbf{y}|} \|\rho(\mathbf{y})\|_{\ell^2} dS(\mathbf{y}) \right\| \leq C\epsilon \|\rho\|.$$

We also observe that

$$\left\| \int_{\partial\Omega} \frac{\delta}{\epsilon^2} |\rho(\mathbf{y})| dS(\mathbf{y}) \right\| \leq \frac{C\delta}{\epsilon^2} |\partial\Omega|^{1/2} \|\rho\|.$$

Hence

$$\begin{aligned} & \left\| \int_{\partial\Omega} T_{jk}(\mathbf{x}, \mathbf{y}; \delta) \rho(\mathbf{y}) dS(\mathbf{y}) - \int_{\partial\Omega} T_{jk}(\mathbf{x}, \mathbf{y}; 0) \rho(\mathbf{y}) dS(\mathbf{y}) \right\| \\ & \leq C \left(\epsilon + \frac{\delta}{\epsilon^2} \right) \|\rho\|, \end{aligned}$$

for some constant C independent of δ, ϵ and ρ . Choosing $\epsilon = \delta^{1/3}$ in the above inequality gives

$$\begin{aligned} & \left\| \int_{\partial\Omega} T_{jk}(\mathbf{x}, \mathbf{y}; \delta) \rho_k(\mathbf{y}) dS(\mathbf{y}) - \int_{\partial\Omega} T_{jk}(\mathbf{x}, \mathbf{y}; 0) \rho_k(\mathbf{y}) dS(\mathbf{y}) \right\| \\ & \leq 2C\delta^{1/3} \|\rho\|. \end{aligned}$$

In particular, the integral operator with kernel $T(\mathbf{x}, \mathbf{y}; 0)$ is the norm limit of the compact operators with kernels $T(\mathbf{x}, \mathbf{y}; \delta)$, and hence is compact. \square

Remark. Up to rotations and translations, the functions $G^{B,2}$ and $G^{B,3}$ defined above are the Boussinesq-Cerruti solutions [12, 19] for the half-plane problem. In [57] Mindlin derived a more general formula for the Green's function in a halfspace with zero normal boundary stress. Taking the limit as the source approaches the boundary recovers $G^{B,2}$ and $G^{B,3}$.

3. STRING KERNEL REPRESENTATIONS

Intuitively, the functions $G^{B,2}$ and $G^{B,3}$ defined in the previous section are ideal candidates from which to construct solutions to equations (1) and (2). Indeed, one is tempted to introduce the ansatzes

$$u_2(\mathbf{x}) = \int_{\partial\Omega} G^{B,2}(\mathbf{x}, \mathbf{y}; \hat{\mathbf{n}}(\mathbf{y})) \rho_2(\mathbf{y}) dS_{\mathbf{y}},$$

$$u_3(\mathbf{x}) = \int_{\partial\Omega} G^{B,3}(\mathbf{x}, \mathbf{y}; \hat{\mathbf{n}}(\mathbf{y})) \rho_3(\mathbf{y}) \, dS_{\mathbf{y}},$$

for the two-dimensional and three-dimensional problems, respectively, where ρ_2, ρ_3 are unknown densities on the boundary $\partial\Omega$, and the vectors $\hat{\mathbf{n}}$ in the functions $G^{B,2}$ and $G^{B,3}$ are chosen to point in the direction of the outward facing normal of Ω at \mathbf{y} . For exterior problems the directions of $\hat{\mathbf{n}}$ should be flipped.

Unfortunately, the branch cuts of $G^{B,2}$ and the line singularities of $G^{B,3}$ mean that for any exterior problem, or interior problems on sufficiently non-convex domains, the functions u_2 and u_3 will not satisfy the PDE $L[u] = 0$. In this section we construct new functions $K^{B,2}$ and $K^{B,3}$ which have the same singularities as $G^{B,2}$ and $G^{B,3}$ near \mathbf{y} , but possess singularities or discontinuities only on the *finite* line segment $\ell_{\mathbf{y}, \hat{\mathbf{v}}, h} := \{\mathbf{x} = \mathbf{y} + t\hat{\mathbf{v}} \mid t \in [0, h]\}$, where $h > 0$ is a free parameter. The construction is based on the observation (see [29] for example), that certain derivatives of $G^{B,2}$ and $G^{B,3}$ do not exhibit these line singularities. Appropriate kernels can thus be constructed by taking definite integrals over finite line segments. In two dimensions this is given by the following lemma which follows immediately from the definition of $G^{B,2}$.

Lemma 3.1. *The function*

$$\begin{aligned} \hat{\mathbf{v}} \cdot \nabla_{\mathbf{y}} G^{B,2}(\mathbf{x}, \mathbf{y}; \hat{\mathbf{v}}) &= \frac{1}{2\pi\mu} \left[-\frac{\mathbf{r} \cdot \hat{\mathbf{v}}}{\alpha r^2} \mathbf{I}_2 + \frac{\hat{\mathbf{v}} \mathbf{r}^T + \mathbf{r} \hat{\mathbf{v}}^T}{r^2} - \frac{(\mathbf{r} \cdot \hat{\mathbf{v}}) \mathbf{r} \mathbf{r}^T}{r^4} \right] \\ &\quad + \frac{1}{2\pi\mu} \frac{1 - \alpha \hat{\mathbf{v}}^\perp \cdot \mathbf{r}}{\alpha} \frac{\mathbf{r}}{r^2} \begin{pmatrix} 0 & 1 \\ -1 & 0 \end{pmatrix}, \end{aligned}$$

has a removable singularity on the line $\{\mathbf{x} = \mathbf{y} + t\hat{\mathbf{v}} \mid t \in (0, \infty)\}$, and satisfies $L[\hat{\mathbf{v}} \cdot \nabla_{\mathbf{y}} G^{B,2}](\mathbf{x}) = 0$ for all $\mathbf{x} \neq \mathbf{y}$.

The following corollary follows immediately from the previous lemma, and gives the construction of a suitable function $K^{B,2}$ having the desired properties.

Corollary 3.1.1. *Defining $K^{B,2}$ by*

$$\begin{aligned} K^{B,2}(\mathbf{x}, \mathbf{y}; \hat{\mathbf{v}}, h) &= - \int_0^h \hat{\mathbf{v}} \cdot \nabla_{\mathbf{y}} G^{B,2}(\mathbf{x}, \mathbf{y} + t\hat{\mathbf{v}}; \hat{\mathbf{v}}) \, dt \\ &= G^{B,2}(\mathbf{x}, \mathbf{y}; \hat{\mathbf{v}}) - G^{B,2}(\mathbf{x}, \mathbf{y} + h\hat{\mathbf{v}}; \hat{\mathbf{v}}), \end{aligned}$$

gives a function which satisfies $L[K^{B,2}] = 0$ everywhere except the line segment $\ell_{\mathbf{y}, \hat{\mathbf{v}}, h}$. Moreover, $K^{B,2}(\mathbf{x}, \mathbf{y}; \hat{\mathbf{v}}, h) - G^{B,2}(\mathbf{x}, \mathbf{y}; \hat{\mathbf{v}})$ is a smooth function of \mathbf{x} in a neighborhood of \mathbf{y} .

Similar results hold in three dimensions, though an extra derivative is required.

Lemma 3.2. *The function*

$$(7) \quad \begin{aligned} \hat{\mathbf{v}} \cdot \nabla_{\mathbf{y}} (\hat{\mathbf{v}} \cdot \nabla_{\mathbf{y}} G^{B,3})(\mathbf{x}, \mathbf{y}; \hat{\mathbf{v}}) &= \frac{1}{4\pi\mu} \hat{\mathbf{v}} \cdot \nabla_{\mathbf{y}} \hat{\mathbf{v}} \cdot \nabla_{\mathbf{y}} \left[\frac{\mathbf{I}_3}{r} + \frac{\mathbf{r}\mathbf{r}^T}{r^3} \right] \\ &+ \frac{1}{4\pi\mu} \frac{1-\alpha}{\alpha} \left[\frac{\mathbf{I}_3}{r^3} - 2 \frac{\hat{\mathbf{v}}\hat{\mathbf{v}}^T}{r^3} - 3 \frac{Q_{\hat{\mathbf{v}}}\mathbf{r}\mathbf{r}^T Q_{\hat{\mathbf{v}}}}{r^5} \right. \\ &\left. - 3(\mathbf{r} \cdot \hat{\mathbf{v}}) \frac{\mathbf{r}\hat{\mathbf{v}}^T - \hat{\mathbf{v}}\mathbf{r}^T - (\mathbf{r} \cdot \hat{\mathbf{v}})\hat{\mathbf{v}}\hat{\mathbf{v}}^T}{r^5} \right], \end{aligned}$$

has a removable singularity on the line $\{\mathbf{x} = \mathbf{y} + t\hat{\mathbf{v}} \mid t \in (0, \infty)\}$, and satisfies $L[\hat{\mathbf{v}} \cdot \nabla_{\mathbf{y}} \hat{\mathbf{v}} \cdot \nabla_{\mathbf{y}} G^{B,3}](\mathbf{x}) = 0$ for all $\mathbf{x} \neq \mathbf{y}$.

As for the two-dimensional case, the above lemma motivates the definition of a function, $K^{B,3}$, defined by integration of (7) over a finite line segment.

Corollary 3.2.1. *Let $K^{B,3}$ be the function defined by*

$$(8) \quad \begin{aligned} K^{B,3}(\mathbf{x}, \mathbf{y}; \hat{\mathbf{v}}, h) &= \int_0^h \int_s^h \hat{\mathbf{v}} \cdot \nabla_{\mathbf{y}} (\hat{\mathbf{v}} \cdot \nabla_{\mathbf{y}} G^{B,3}(\mathbf{x}, \mathbf{y} + t\hat{\mathbf{v}}; \hat{\mathbf{v}})) dt ds \\ &= \int_0^h t \hat{\mathbf{n}} \cdot \nabla_{\mathbf{y}} (\hat{\mathbf{v}} \cdot \nabla_{\mathbf{y}} G^{B,3}(\mathbf{x}, \mathbf{y} + t\hat{\mathbf{v}}; \hat{\mathbf{v}})) dt \\ (9) \quad &= G^{B,3}(\mathbf{x}, \mathbf{y}; \hat{\mathbf{v}}) - G^{B,3}(\mathbf{x}, \mathbf{y} + h\hat{\mathbf{v}}; \hat{\mathbf{v}}) + h \hat{\mathbf{v}} \cdot \nabla_{\mathbf{y}} G^{B,3}(\mathbf{x}, \mathbf{y} + h\hat{\mathbf{v}}; \hat{\mathbf{v}}). \end{aligned}$$

Then $L[K^{B,3}] = 0$ everywhere except the line segment $\ell_{\mathbf{y}, \hat{\mathbf{v}}, h}$ and $K^{B,3}(\mathbf{x}, \mathbf{y}; \hat{\mathbf{v}}, h) - G^{B,3}(\mathbf{x}, \mathbf{y}; \hat{\mathbf{v}})$ is a smooth function of \mathbf{x} in a neighborhood of \mathbf{y} .

It will also be convenient to have the expression for the stress tensors associated with $\hat{\mathbf{v}} \cdot \nabla_{\mathbf{y}} G^{B,3}$ and $\hat{\mathbf{v}} \cdot \nabla_{\mathbf{y}} \hat{\mathbf{v}} \cdot \nabla_{\mathbf{y}} G^{B,3}$. Tedious but straightforward calculations yield

$$\begin{aligned} -\sigma[\hat{\mathbf{v}} \cdot \nabla_{\mathbf{y}} G^{B,3}(\cdot, \mathbf{y}, \hat{\mathbf{v}})]_{ijk}(\mathbf{x}) &= -6 \frac{\mathbf{r}_i \mathbf{r}_j \hat{\mathbf{v}}_k + \mathbf{r}_i \hat{\mathbf{v}}_j \mathbf{r}_k + \hat{\mathbf{v}}_i \mathbf{r}_j \mathbf{r}_k}{4\pi r^5} + 30 \frac{\mathbf{r}_i \mathbf{r}_j \mathbf{r}_k (\mathbf{r} \cdot \hat{\mathbf{v}})}{4\pi r^7} \\ &+ \frac{1}{4\pi} \frac{1-\alpha}{\alpha} \left\{ -2 \frac{(Q\mathbf{r})_i (Q\mathbf{r})_j \hat{\mathbf{v}}_k (R+2r)}{r^3 R^3} \right. \\ &+ 2 \frac{(Q\mathbf{r})_i (Q\mathbf{r})_j \mathbf{r}_k}{r^5 R^3} (2r^2 + 3rR + 3R^2) + 2 \frac{Q_{i,j} \hat{\mathbf{v}}_k}{r R^2} \\ &- 2 \frac{R+r}{r^3 R^2} (Q_{i,k} (Q\mathbf{r})_j + Q_{j,k} (Q\mathbf{r})_i + Q_{i,j} \mathbf{r}_k) \\ &\left. + 2 \frac{Q_{i,j} \hat{\mathbf{v}}_k}{r^3} - \frac{6(\hat{\mathbf{v}} \cdot \mathbf{r}) Q_{i,j} \mathbf{r}_k}{r^5} \right\}. \end{aligned}$$

and

$$\begin{aligned} \sigma[\hat{\mathbf{v}} \cdot \nabla_{\mathbf{y}} \hat{\mathbf{v}} \cdot \nabla_{\mathbf{y}} G^{B,3}(\cdot, \mathbf{y}, \hat{\mathbf{v}})]_{ijk}(\mathbf{x}) &= -12 \frac{\mathbf{r}_i \hat{\mathbf{v}}_j \hat{\mathbf{v}}_k + \hat{\mathbf{v}}_i \mathbf{r}_j \hat{\mathbf{v}}_k + \hat{\mathbf{v}}_i \hat{\mathbf{v}}_j \mathbf{r}_k}{4\pi r^5} + 30 \frac{\mathbf{r}_i \mathbf{r}_j \mathbf{r}_k}{4\pi r^7} \\ &+ 60 \frac{(\mathbf{r}_i \mathbf{r}_j \hat{\mathbf{v}}_k + \mathbf{r}_i \hat{\mathbf{v}}_j \mathbf{r}_k + \hat{\mathbf{v}}_i \mathbf{r}_j \mathbf{r}_k)(\mathbf{r} \cdot \hat{\mathbf{v}})}{4\pi r^7} - 210 \frac{\mathbf{r}_i \mathbf{r}_j \mathbf{r}_k (\mathbf{r} \cdot \hat{\mathbf{v}})^2}{4\pi r^9} \\ &+ \frac{1}{4\pi} \frac{1-\alpha}{\alpha} \left\{ 30 \frac{(Q\mathbf{r})_i (Q\mathbf{r})_j \mathbf{r}_k}{r^7} - 6 \frac{Q_{i,k} (Q\mathbf{r})_j + Q_{j,k} (Q\mathbf{r})_i}{r^5} \right. \end{aligned}$$

$$\left. -12 \frac{Q_{i,j} \hat{\mathbf{v}}_k(\mathbf{r} \cdot \hat{\mathbf{v}})}{r^5} - 12 \frac{Q_{i,j} \mathbf{r}_k}{r^5} + 30 \frac{Q_{i,j} \mathbf{r}_k (\mathbf{r} \cdot \hat{\mathbf{v}})^2}{r^7} \right\},$$

where, for ease of exposition, we have suppressed the dependence of Q on $\hat{\mathbf{v}}$.

In the following, we define the functions $\Sigma^{B,2}$ and $\Sigma^{B,3}$ by

$$\Sigma^{B,2}(\mathbf{x}, \mathbf{y}; h) := \hat{\mathbf{n}}(\mathbf{x}) \cdot \sigma[K^{B,2}(\cdot, \mathbf{y}; \hat{\mathbf{n}}(\mathbf{y}), h)](\mathbf{x}),$$

and

$$\Sigma^{B,3}(\mathbf{x}, \mathbf{y}; h) := \hat{\mathbf{n}}(\mathbf{x}) \cdot \sigma[K^{B,3}(\cdot, \mathbf{y}; \hat{\mathbf{n}}(\mathbf{y}), h)](\mathbf{x}),$$

respectively, and choose $h = h(\mathbf{y})$ to be a smooth non-vanishing function of \mathbf{y} sufficiently small so that for each $\mathbf{y} \in \partial\Omega$, the line segment $\ell_{\mathbf{y}, \hat{\mathbf{n}}, h(\mathbf{y})}$ only touches the surface $\partial\Omega$ at the single point \mathbf{y} .

We summarize the previous results in the following theorems.

Theorem 3.3. *For a domain Ω with smooth boundary $\partial\Omega$ in \mathbb{R}^d , $d = 2, 3$, let $h : \partial\Omega \rightarrow \mathbb{R}^+$ be a smooth function such that for each $\mathbf{y} \in \partial\Omega$, the intersection of the line segment $\ell_{\mathbf{y}, \hat{\mathbf{n}}(\mathbf{y}), h(\mathbf{y})}$ with $\partial\Omega$ is $\{\mathbf{y}\}$. For $\rho \in L^2(\partial\Omega; \mathbb{R}^d)$,*

$$\begin{aligned} & \lim_{\delta \rightarrow 0^+} \hat{\mathbf{n}}_i(\mathbf{x}) \sigma \left[\int K^{B,d}(\cdot, \mathbf{y}; \hat{\mathbf{n}}(\mathbf{y}), h(\mathbf{y})) \rho(\mathbf{y}) \, dS(\mathbf{y}) \right]_{ijk} (\mathbf{x} - \delta \hat{\mathbf{n}}) \\ &= \rho_j(\mathbf{x}) + \int \Sigma_{jk}^{B,d}(\mathbf{x}, \mathbf{y}; h(\mathbf{y})) \rho_k(\mathbf{y}) \, dS(\mathbf{y}), \end{aligned}$$

in an L^2 sense. Moreover, the integral operator on the right-hand side is compact from $L^2(\partial\Omega; \mathbb{R}^d)$ to itself.

Proof. From Corollary 3.1.1 in 2D and Corollary 3.2.1 in 3D, it is clear that $K^{B,d}(\mathbf{x}, \mathbf{y}, \hat{\mathbf{n}}(\mathbf{y}), h(\mathbf{y})) - G^{B,d}(\mathbf{x}, \mathbf{y}, \hat{\mathbf{n}}(\mathbf{y}))$ is smooth for $\mathbf{x} \in \Omega$ sufficiently close to $\mathbf{y} \in \partial\Omega$. Moreover, $K^{B,d}(\mathbf{x}, \mathbf{y}, \hat{\mathbf{n}}(\mathbf{y}), h(\mathbf{y}))$ and $G^{S,d}$ are smooth in Ω outside of any ball containing \mathbf{y} . Next we write

$$\begin{aligned} K^{B,d} &= 2G^{S,d} + G^{D,d} \chi_{\beta'}(\mathbf{x} - \mathbf{y}) + (K^{B,d} - 2G^{S,d} - G^{D,d} \chi_{\beta'}(\mathbf{x} - \mathbf{y})), \\ &= 2G^{S,d} + G^{D,d} \chi_{\beta'}(\mathbf{x} - \mathbf{y}) + (K^{B,d} - 2G^{S,d} - G^{D,d}) \chi_{\beta'}(\mathbf{x} - \mathbf{y}) \\ &\quad + (K^{B,d} - 2G^{S,d})(1 - \chi_{\beta'}(\mathbf{x} - \mathbf{y})) \\ &= 2G^{S,d} + G^{D,d} \chi_{\beta'}(\mathbf{x} - \mathbf{y}) + \mathcal{R}. \end{aligned}$$

By construction, both terms comprising \mathcal{R} are smooth in $\bar{\Omega}$. It follows immediately that

$$\begin{aligned} & \lim_{\delta \rightarrow 0^+} \hat{\mathbf{n}}(\mathbf{x}) \cdot \sigma \left[\int \mathcal{R}(\cdot, \mathbf{y}) \rho(\mathbf{y}) \, dS(\mathbf{y}) \right] (\mathbf{x} - \delta \hat{\mathbf{n}}) \\ &= \int \hat{\mathbf{n}}(\mathbf{x}) \cdot \sigma[\mathcal{R}(\cdot, \mathbf{y})](\mathbf{x}) \rho(\mathbf{y}) \, dS(\mathbf{y}). \end{aligned}$$

Applying Theorem 2.1 to $G^{S,d}$ and Theorem 2.2 to $G^{D,d}$ gives the required result. \square

We collect the preceding results in the following theorem.

Theorem 3.4. *Let Ω be a domain in \mathbb{R}^d , $d = 2, 3$ with smooth boundary $\partial\Omega$. For a right-hand side $f \in L^2(\partial\Omega; \mathbb{R}^d)$, if we introduce the ansatz*

$$u_j(\mathbf{x}) = \int_{\partial\Omega} K_{jk}^{B,d}(\mathbf{x}, \mathbf{y}; \hat{\mathbf{n}}(\mathbf{y}), h(\mathbf{y})) \rho_k(\mathbf{y}) \, dS(\mathbf{y}),$$

then the density ρ satisfies the integral equation

$$(10) \quad \rho_j(\mathbf{x}) + \int_{\partial\Omega} \Sigma_{jk}^{B,d}(\mathbf{x}, \mathbf{y}; h(\mathbf{y})) \rho_k(\mathbf{y}) \, dS(\mathbf{y}) = f(\mathbf{x}).$$

Moreover, (10) is a Fredholm integral equation of the second kind.

Remark. Recall that the traction boundary value problem in elastostatics has a finite-dimensional nullspace corresponding to rigid body motions. The dimensionality of the nullspace is 3 in two dimensions, and 6 in three dimensions, which is inherited by equation 10. These nullspaces can be eliminated by enforcing that the density ρ satisfy 3 additional constraints in two dimensions and 6 additional constraints in three dimensions, as is done for mobility and interior traction problems in Stokes flow, see [63, 21], for example.

3.1. Limiting behavior of the integral equations. Here we analyze the incompressible limit corresponding to taking $\lambda \rightarrow \infty$, or equivalently, $\alpha \rightarrow 1^-$, with μ fixed. We start with the two-dimensional case. In this limit, for any \mathbf{x} not on the half-line emanating from \mathbf{y} in the direction $\hat{\mathbf{n}}$, we have $\lim_{\alpha \rightarrow 1} G^{B,2}(\mathbf{x}, \mathbf{y}; \hat{\mathbf{v}}) = 2 G^{S,2}(\mathbf{x}, \mathbf{y})$. Turning to the normal stress, away from the half-line we observe that $\hat{\mathbf{v}} \cdot \sigma[G^{B,2}] = 2\hat{\mathbf{v}} \cdot \sigma[G^{S,2}]$. In particular, the integral operator in the 2D integral equation (10) is independent of α . Explicitly, (10) can be written as

$$(11) \quad \frac{1}{2}\rho_i(\mathbf{x}) - \frac{1}{\pi} \int_{\partial\Omega} \hat{\mathbf{n}}_j(\mathbf{x}) \frac{(x_i - y_i)(x_j - y_j)(x_k - y_k)}{|\mathbf{x} - \mathbf{y}|^4} \rho_k(\mathbf{y}) \, dS(\mathbf{y})$$

$$(12) \quad = \frac{1}{2}f_i(\mathbf{x}) - \frac{1}{\pi} \int_{\partial\Omega} \hat{\mathbf{n}}_j(\mathbf{x}) \frac{(x_i - y'_i)(x_j - y'_j)(x_k - y'_k)}{|\mathbf{x} - \mathbf{y}'|^4} \rho_k(\mathbf{y}) \, dS(\mathbf{y}),$$

with $\mathbf{y}' = \mathbf{y} + h(\mathbf{y})\hat{\mathbf{n}}(\mathbf{y})$. The left-hand side of the previous equation is just the integral equation for solving the traction boundary value problem when the velocity is represented using the single layer potential for Stokes flow in two dimensions, while the integral operator on the right-hand side has a smooth kernel and so is compact. Hence, for any α , (10) is a compact perturbation of the surface traction integral equation and moreover, if (10) is solvable for one α then it is solvable for every α , (in appropriate spaces which handle the non-uniqueness corresponding to rigid body motions, see Remark 3).

Next we turn to 3D. Suppose that \mathbf{x} is not on the half-line emanating from \mathbf{y} and pointing in the direction $\hat{\mathbf{n}}$. It follows immediately from the definition of $\Sigma^{B,3}$ and Theorem 3.3 that

$$\Sigma_{jk}^{B,3}(\mathbf{x}, \mathbf{y}, h(\mathbf{y})) = 2 [\hat{\mathbf{n}}_i(\mathbf{x})\sigma[G^{S,3}(\mathbf{x}, \mathbf{y})]_{ijk} - \hat{\mathbf{n}}_i(\mathbf{x})\sigma[G^{S,3}(\mathbf{x}, \mathbf{y}')]_{ijk}]$$

$$+ (1 - \alpha)K_{j,k}(\mathbf{x}, \mathbf{y}),$$

where $K_{j,k}$ is a kernel corresponding to a compact operator, uniformly bounded for $\delta > 0$ sufficiently small. In particular, (10) is a compact perturbation of the integral equation arising in the traction boundary value problem when the velocity is represented using the Stokes layer potential, and in the limit as $\alpha \rightarrow 1^-$ the integral operator converges to

$$\begin{aligned} & \frac{1}{2}\rho_i(\mathbf{x}) - \frac{6}{8\pi} \int_{\partial\Omega} \hat{\mathbf{n}}_j(\mathbf{x}) \frac{(x_i - y_i)(x_j - y_j)(x_k - y_k)}{|\mathbf{x} - \mathbf{y}|^5} \rho_k(\mathbf{y}) \, dS(\mathbf{y}) \\ (13) \quad & = \frac{1}{2}f_i(\mathbf{x}) - \frac{6}{8\pi} \int_{\partial\Omega} \hat{\mathbf{n}}_j(\mathbf{x}) \frac{(x_i - y'_i)(x_j - y'_j)(x_k - y'_k)}{|\mathbf{x} - \mathbf{y}'|^5} \rho_k(\mathbf{y}') \, dS(\mathbf{y}'). \end{aligned}$$

In particular, if (13) is invertible then (10) will be invertible for all α sufficiently close to 1.

4. NUMERICAL APPARATUS

In this section we briefly sketch relevant details for the discretization and solution of the integral equation (10). A nice feature of our approach is that only minor modifications are required in order to use standard integral equations toolboxes, chunkIE [6] in two dimensions and fmm3DBIE [5] in three dimensions. Moreover, the kernels used in both our integral representation and the corresponding integral equations can be applied quickly via a small extension to the standard fast multipole method toolboxes [3].

4.1. Evaluation of the kernels. In two dimensions, the kernel $\Sigma^{B,2}(\cdot, \mathbf{y}; h(\mathbf{y}))$ is only singular at \mathbf{y} and $\mathbf{y} + h(\mathbf{y})\hat{\mathbf{n}}(\mathbf{y})$. Indeed, combining the identity (4) with Corollary 3.1.1, we obtain

$$\Sigma^{B,2}(\mathbf{x}, \mathbf{y}, h(\mathbf{y})) = -2 \frac{(\mathbf{r} \cdot \hat{\mathbf{n}}(\mathbf{x}))r_j r_k}{\pi r^4} + 2 \frac{(\mathbf{r}' \cdot \hat{\mathbf{n}}(\mathbf{x}))r'_j r'_k}{\pi (r')^4},$$

with $\mathbf{r}' = \mathbf{x} - \mathbf{y} - h\hat{\mathbf{n}}(\mathbf{y})$. By construction, for a given geometry we can choose $h(\mathbf{y})$ so that $r' = |\mathbf{r}'|$ is bounded away from zero. In particular, the second term can be stably evaluated with minimal loss of accuracy due to catastrophic cancellations. The first term arises in other boundary integral equations, see [61] for example, and can be evaluated using standard methods. Indeed, we observe that if $\partial\Omega$ is smooth, and $\mathbf{r}(t)$ is an arclength parameterization of $\partial\Omega$, then $\mathbf{r}(t) - \mathbf{r}(s) = (t - s)\boldsymbol{\tau}(t) + \frac{\kappa}{2}(t - s)^2\hat{\mathbf{n}}(t) + O((t - s)^3)$. Then, the first term in the kernel becomes

$$-\kappa \frac{r_j r_k}{r^2} + O(|\mathbf{r}|),$$

for $\mathbf{x}, \mathbf{y} \in \partial\Omega$. Using this approximation, for $|\mathbf{x} - \mathbf{y}|$ small enough the kernel can be stably evaluated. In principle, higher order expansions can be used — these involve evaluating higher order derivatives of the normal vector.

For $K^{B,2}$, similar reasoning applies. In principle, for $\mathbf{x} \approx \mathbf{y} + t\hat{\mathbf{n}}(\mathbf{y})$ with $t > 0$ sufficiently large, one will get catastrophic cancellation involving the

difference of the kernels. In practice, this will not be significant except when evaluating points very far away, where other formulas can be used.

In three dimensions, singularities are present on the line segments $\ell_{\mathbf{y},\hat{\mathbf{n}},h}$ both in the integral equation kernel $\Sigma^{B,3}(\cdot, \mathbf{y}; h(\mathbf{y}))$ and the kernel used in the representation $K^{B,3}$. In particular, if (9) is used to calculate both $\Sigma^{B,3}$ and $K^{B,3}$ then when $\mathbf{x} \approx \mathbf{y} + t\hat{\mathbf{n}}(\mathbf{y})$ with $t > h(\mathbf{y})$, catastrophic cancellations will occur, even though the kernels are smooth and decaying in $|\mathbf{x} - \mathbf{y}|$. To avoid this issue, for $|\mathbf{x} - \mathbf{y}| > h(\mathbf{y})$ we instead use the integral representation of $K^{B,3}$ given in (8). From (7) we note that the integrand is smooth for \mathbf{x} away from $\ell_{\mathbf{y},\hat{\mathbf{n}}(\mathbf{y}),h(\mathbf{y})}$. It follows that the integral in (8) may be computed using a standard Gauss-Legendre quadrature with an order which depends only logarithmically on the desired accuracy.

4.2. Discretization of the integral equations. As mentioned above, the boundary integral equation (10) is amenable to standard discretization and quadrature methods. Here we use the software package chunkIE [6] in two dimensions, and fmm3DBIE [5] in three dimensions, which discretize and solve integral equations using a patch-based collocation scheme [35]. In particular, both the geometry and unknowns are represented using piecewise polynomial expansions. For curves in two dimensions these quantities are interpolated from Gauss-Legendre quadrature nodes, while for surfaces in three dimensions they are interpolated from Vioreanu-Rokhlin nodes [69, 71]. High-order quadratures for weakly-singular integral operators are constructed via *generalized Gaussian quadrature* [13, 53, 73].

4.3. Fast algorithms. As is typical for boundary integral equations, discretizing (10) yields a dense linear system. In either case, however, both the application of these matrices and their inversion can be accelerated using existing machinery with only minor modifications. Here we briefly sketch the necessary observations, deferring a complete 3D implementation to a subsequent paper.

In two dimensions, the kernel appearing in the integral equation differs from the traction of the 2D Stokes single-layer by only a smooth function (which can itself be written as the traction of the Stokes single-layer from a suitable source). Thus, only two Stokeslet evaluations are required per source. Existing fast iterative solvers based on the 2D Stokes FMM [28], and fast direct solvers based on hierarchical skeletonization [54, 33, 67, 56, 22], therefore apply essentially unchanged.

In three dimensions, Corollary 3.2.1 expresses each entry of $\Sigma^{B,3}(\mathbf{x}, \mathbf{y}; h)$ as a line integral over $\ell_{\mathbf{y},\hat{\mathbf{n}},h}$ of a linear combination of terms

$$(14) \quad f(\mathbf{x}) g(\mathbf{y}) \partial_{\mathbf{x}}^{\alpha} \frac{1}{|\mathbf{x} - \mathbf{y}|}, \quad |\alpha| \leq 3,$$

with f, g explicit scalar functions. For $|\mathbf{x} - \mathbf{y}|$ large compared to h , the line integral is captured to high precision by a fixed-order Gauss-Legendre rule (order 16 in our experiments), reducing each far-field interaction to a sum

of terms of the form (14). Kernels of this type can be applied quickly using the standard 3D Laplace FMM [36, 3]. For $|\mathbf{x} - \mathbf{y}|$ comparable to or smaller than h , the kernel is evaluated directly via (9) together with standard near-singular and self-interaction quadratures. This yields an $O(N)$ algorithm for applying the system matrix, provided the strings are short compared with the FMM leaf-box size, a condition enforceable by sufficient tree refinement. An analogous constraint on string endpoints applies to hierarchical direct solvers, where long strings can destroy the low-rank structure of far-field blocks. Perhaps the most closely related existing construction is [29], which treats the case of infinite, uniformly vertical strings.

4.4. Heuristics for the choice of h . In two dimensions there is additional flexibility which greatly simplifies matters. For ease of exposition we focus on the interior problem for a simply connected domain Ω , though an almost identical approach can be used for exterior problems and non-simply connected Ω . For fixed \mathbf{x} and \mathbf{y} we observe that $K^{B,2}(\mathbf{x}, \mathbf{y}; \hat{\mathbf{n}}, h)$ has a branch cut c along $\ell_{\mathbf{y}, \hat{\mathbf{n}}, h}$ connecting \mathbf{y} to $\mathbf{y}_s = \mathbf{y} + h\hat{\mathbf{n}}$. The remainder of the kernel is smooth in \mathbf{x} except at \mathbf{y} and \mathbf{y}_s .

Clearly, one is free to continuously deform c as long as it does not pass through \mathbf{x} . Let \mathbf{y}_* be a point in Ω^c connected to \mathbf{y} and \mathbf{y}_s by smooth curves $c', c'' \subset \bar{\Omega}^c$, respectively, such that $c' \cup c''$ is continuously deformable to $\ell_{\mathbf{y}, \hat{\mathbf{n}}, h}$ while remaining in Ω^c . Then

$$\begin{aligned} K^{B,2}(\mathbf{x}, \mathbf{y}; \hat{\mathbf{n}}, h) &= (G^{B,2}(\mathbf{x}, \mathbf{y}; c') - G^{B,2}(\mathbf{x}, \mathbf{y}_*; c')) \\ &\quad - (G^{B,2}(\mathbf{x}, \mathbf{y}_*; c'') - G^{B,2}(\mathbf{x}, \mathbf{y}_s; c'')), \end{aligned}$$

where the branch cut in the first term lies along c' and the branch cut in the second term lies along c'' . Here, with some abuse of notation, we replace the vector $\hat{\mathbf{n}}$ in the arguments of $G^{B,2}$ with the curve along which the branch cut lies.

We note that the second term satisfies the homogeneous PDE in Ω , and has smooth normal stress on $\partial\Omega$. Hence, we are free to replace $K^{B,2}$ in our representation with

$$K_{\mathbf{y}_*}^{B,2} := G^{B,2}(\mathbf{x}, \mathbf{y}; c') - G^{B,2}(\mathbf{x}, \mathbf{y}_*; c'),$$

where the branch cut in $G^{B,2}$ lies along c' .

In three dimensions, the optimal choice of h remains something of an open problem. On one hand, if h is chosen too small, then the singularities from each end of the string almost cancel, and the condition number deteriorates. On the other hand, if h is too large then the singularities associated with the far end of the string will lead to nearly singular interactions with other parts of the boundary, requiring finer discretization and possibly again increasing the condition number. In all of the examples considered in this work, we use a fixed string length.

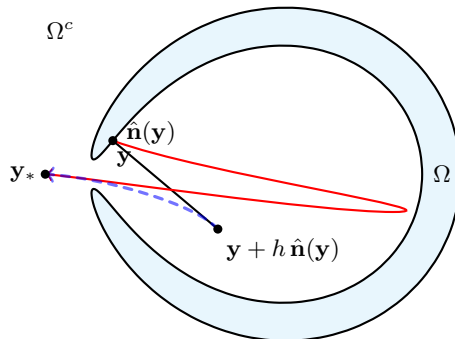


FIGURE 2. The contour-deformation kernel $K_{\mathbf{y}_*}^{B,2}$ on a smooth cavity domain Ω . The black segment is the original truncated string from \mathbf{y} to $\mathbf{y} + h \hat{\mathbf{n}}(\mathbf{y})$, on which $K^{B,2}(\cdot, \mathbf{y}; \hat{\mathbf{n}}, h)$ has its line singularity. The solid red contour is a smooth deformation from \mathbf{y} to a point $\mathbf{y}_* \in \Omega^c$, sweeping through the cavity and out the opening of Ω ; this defines the modified kernel $K_{\mathbf{y}_*}^{B,2}(\mathbf{x}, \mathbf{y}) = G^{B,2}(\mathbf{x}, \mathbf{y}; \hat{\mathbf{n}}(\mathbf{y})) - G^{B,2}(\mathbf{x}, \mathbf{y}_*; \hat{\mathbf{n}}(\mathbf{y}))$. The dashed contour from $\mathbf{y} + h \hat{\mathbf{n}}(\mathbf{y})$ to \mathbf{y}_* is the auxiliary curve used to identify the difference $K_{\mathbf{y}_*}^{B,2} - K^{B,2}$ as an integral that is regular in Ω .

5. NUMERICAL ILLUSTRATIONS

To illustrate the performance of our approach, we consider the solution of the PDE in the interior of a star-shaped geometry (Ω_{star}), and a cavity-like (Ω_{cavity}) domain in two dimensions, and an ellipsoid ($\Omega_{\text{ellipsoid}}$), and a star-shaped torus (Ω_{torus}) in three dimensions. The parametrization of the star-shaped geometry denoted by γ_{star} is given by

$$\gamma_{\text{star}}(t) = (1 + 0.3 \cos(5t)) \begin{bmatrix} \cos(t) \\ \sin(t) \end{bmatrix}, \quad t \in [0, 2\pi).$$

For the cavity domain, suppose $z(t) = x(t) + iy(t)$, $t \in [0, 2\pi)$ is an ellipse centered at $(20, 0)$ with semi-major and minor axis (a, b) . Then

$$\gamma_{\text{cavity}}(t) = \frac{z^{2\zeta}(t)}{\max_{t \in [0, 2\pi)} (|z(t)|^{2\zeta)},$$

with $(a, b, \zeta) = (0.397, 8.02, 3.965)$. The ellipsoid in three dimensions is coordinate-axis aligned with principal semi-axes $(5.1, 1.0, 2.0)$ respectively. Finally, the parametrization for the star-shaped torus denoted by γ_{torus} is given by

$$\gamma_{\text{torus}}(u, v) = \begin{bmatrix} (R_1 + R_3 \cos(3v) + R_2 \cos(u)) \cos(v) \\ (R_1 + R_3 \cos(3v) + R_2 \cos(u)) \sin(v) \\ R_2 \sin(u) \end{bmatrix},$$

with $(u, v) \in [0, 2\pi)^2$, $R_1 = 4$, $R_2 = 1.5$, and $R_3 = 0.25$. We plot the star-shaped domain, the cavity and the star-shaped torus in Figure 3. Unless

stated otherwise, the string length h is 0.1 for examples in two dimensions, and 0.25 for the examples in three dimensions.

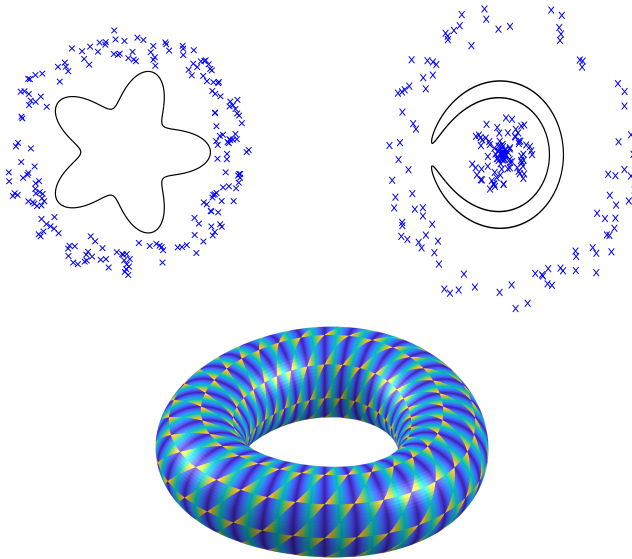


FIGURE 3. Top row: star-shaped domain and cavity domain in two dimensions. The blue crosses indicate the source locations \mathbf{y}_j for generating the exact solution. Bottom row: star-shaped torus domain.

We test the accuracy of the string kernel representation using a known solution in the domain. In two dimensions, suppose $u_{\text{exact}}(\mathbf{x}) = \sum_{j=1}^B G^2(\mathbf{x}, \mathbf{y}_j) \sigma_j$, where the locations of the \mathbf{y}_j are denoted by crosses in Figure 3, the components of $\sigma_j \in \mathbb{R}^2$ are drawn uniformly in $[-0.5, 0.5]$, $G^2(\mathbf{x}, \mathbf{y})$ is the elastostatic Green's function in two dimensions given by

$$G^2(\mathbf{x}, \mathbf{y}) = \frac{1}{2\pi\mu} \left(-(2 - \alpha) \log |\mathbf{x} - \mathbf{y}| I_2 + \alpha \frac{(\mathbf{x} - \mathbf{y})(\mathbf{x} - \mathbf{y})^T}{|\mathbf{x} - \mathbf{y}|^2} \right),$$

$\mu = 1$, and $\lambda = 10$. We then represent the solution and solve the integral equation as described in Theorem 3.4. The integral equation is discretized using chunkIE, and the solution is computed at a grid of targets inside the domain denoted by \mathbf{x}_i , $i = 1, 2, \dots, N_t$. For the star-shaped domain, $N_t = 43410$, and for the cavity $N_t = 14764$. Since the solution is only unique up to a rigid body motion, we first find the best $v_0 \in \mathbb{R}^2, \omega \in \mathbb{R}$, which minimize the residual

$$v_0^*, \omega^* = \operatorname{argmin}_{v_0, \omega} \sum_{i=1}^{N_t} \left| u_{\text{exact}}(\mathbf{x}_i) - u(\mathbf{x}_i) - v_0 - \omega(\mathbf{x}_i - \mathbf{x}_c)^\perp \right|^2,$$

where \mathbf{x}_c is the centroid of the domain given by $\mathbf{x}_c = \int_{\partial\Omega} \mathbf{x} \, dS(\mathbf{x})$, and $\mathbf{x}^\perp = (-x_2, x_1)$. Figure 4 plots the relative pointwise residual $r(\mathbf{x}) = \|u_{\text{exact}}(\mathbf{x}) - u(\mathbf{x}) - v_0^* - \omega^*(\mathbf{x} - \mathbf{x}_c)^\perp\|_{\ell^2} / \|u_{\text{exact}}\|_{\ell^2}$, along with the computed solution $u(\mathbf{x}_i)$ for both the domains.

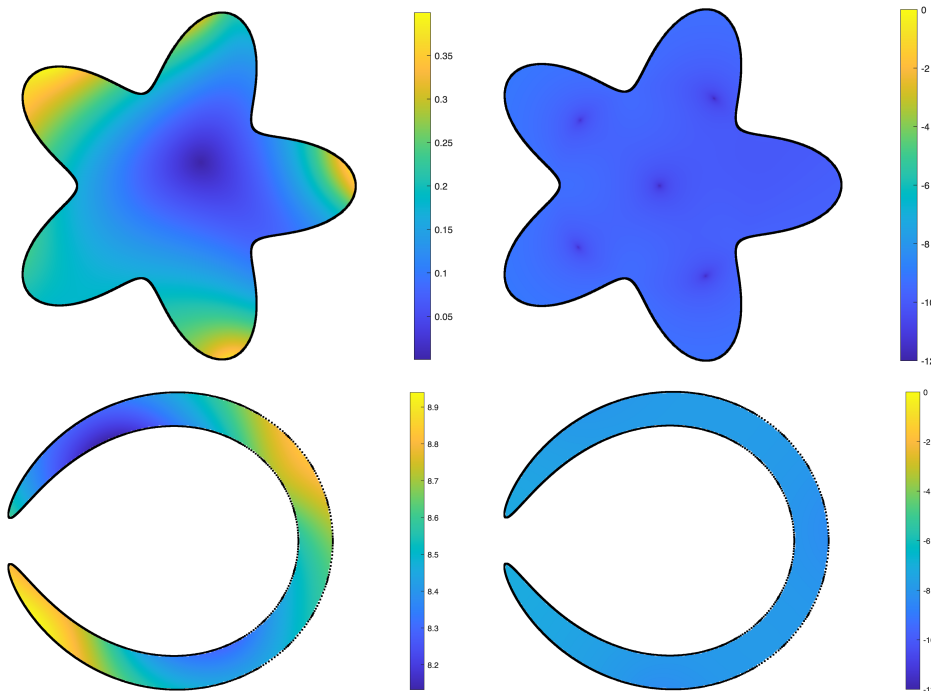


FIGURE 4. Left column: computed solutions $u(\mathbf{x})$ on the star-shaped and cavity domains. Right column: \log_{10} of the relative residual $r(\mathbf{x})$.

In three dimensions, suppose $u_{\text{exact}}(\mathbf{x}) = G^3(\mathbf{x}, \mathbf{y}_0)\sigma_0$, where $\mathbf{y}_0 = (3.1, 3.19, 10.19)$, $\sigma_0 = 10^3(1.1, 2.1, 0.3)$, $G^3(\mathbf{x}, \mathbf{y})$ is the elastostatic Green's function in three dimensions given by

$$G^3(\mathbf{x}, \mathbf{y}) = \frac{1}{4\pi\mu} \left(\frac{(2-\alpha)}{|\mathbf{x}-\mathbf{y}|} I_3 + \alpha \frac{(\mathbf{x}-\mathbf{y})(\mathbf{x}-\mathbf{y})^T}{|\mathbf{x}-\mathbf{y}|^3} \right),$$

$\lambda = 1$, and $\mu = 1$. Following a procedure similar to the one discussed above, we test the accuracy of our solver in three dimensions. The linear system is formed densely and solved using GMRES until a relative residual of 10^{-10} is reached. In Table 1, we illustrate high-order convergence, when the geometries were discretized using 5th order patches and 7th order patches. The reported error is the ℓ^2 norm of the residual $r(\mathbf{x}_i) = u_{\text{exact}}(\mathbf{x}_i) - u(\mathbf{x}_i) - v_0^* - \omega^* \times (\mathbf{x}_i - \mathbf{x}_c)$ at 200 random targets \mathbf{x}_i inside the domain, relative to the norm of the boundary data, $\sigma[u_{\text{exact}}]$. In all cases, the number of GMRES iterations required is independent of the mesh size, indicating a

mesh-independent condition number. In all examples, we eventually observe the expected order of convergence.

Geometry	N_{patches}	n_{order}	n_{iter}	$\frac{\ r\ _{\ell^2}}{\ \sigma[u_{\text{exact}}]\ _{L^2}}$	Empirical convergence order
Ellipsoid	56	5	211	2.7×10^{-2}	
Ellipsoid	224	5	206	2.4×10^{-2}	0.15
Ellipsoid	504	5	190	7.7×10^{-4}	8.49
Ellipsoid	896	5	187	2.0×10^{-4}	4.66
Ellipsoid	56	7	220	2.5×10^{-2}	
Ellipsoid	224	7	190	1.5×10^{-3}	4.03
Ellipsoid	504	7	187	3.9×10^{-5}	9.04
Ellipsoid	896	7	186	2.6×10^{-6}	9.39
Star-shaped torus	128	5	284	3.6×10^{-2}	
Star-shaped torus	512	5	271	2.6×10^{-3}	3.83
Star-shaped torus	1152	5	260	5.8×10^{-4}	3.68
Star-shaped torus	2048	5	257	1.0×10^{-4}	6.05
Star-shaped torus	128	7	286	4.7×10^{-3}	
Star-shaped torus	512	7	263	2.4×10^{-4}	4.27
Star-shaped torus	1152	7	257	2.5×10^{-5}	5.62
Star-shaped torus	2048	7	253	1.3×10^{-6}	10.16

TABLE 1. Convergence results for the ellipsoid and star-shaped torus in three dimensions. N_{patches} is the number of patches in the discretization, n_{order} is the order of discretization on each patch, n_{iter} is the number of GMRES iterations required to converge to a relative residual of 10^{-10} , and $\|r\|_{\ell^2}/\|\sigma[u_{\text{exact}}]\|_{L^2(\partial\Omega;\mathbb{R}^d)}$ is a measure of the relative error. Finally, in the last column, we give the implied order of convergence.

Next, we demonstrate the stability of the string kernel integral equation formulation in the Stokes limit. In two dimensions, the condition number is trivially independent of λ since the kernel of the integral equation, $\sigma[K^{B,2}]$ does not depend on λ . In three dimensions, we illustrate the behavior in this limit numerically by computing the condition numbers of the discretized linear systems for an ellipsoid with principal semi-axes 2, 1, 2 as a function of $\lambda \in (10^{-5}, 10^8)$ ($\lambda \rightarrow \infty$ corresponds to the Stokes limit), see Figure 5. The discrete linear systems were ℓ^2 scaled to obtain a closer approximation of the underlying physical condition number [13]. We observe that the condition number for our representations is practically independent of λ . The ratio of the maximum to minimum condition number over the range of λ is 1.63.

The condition number is sensitive to both the choice of the string length h , and the orientation vector $\hat{\mathbf{v}}$. In Figure 6, we plot the condition number as a function of h on the ellipsoid with principal semi-axes (2,1,2) with $\hat{\mathbf{v}} = \hat{\mathbf{n}}$,

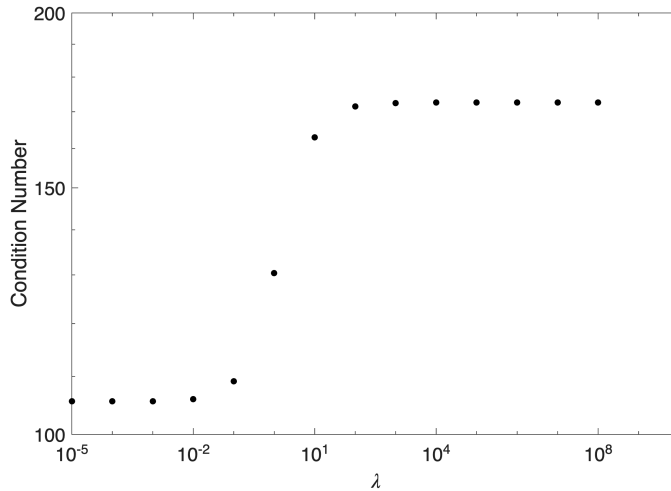


FIGURE 5. Condition number as a function of λ for an ellipsoid with principal semi-axes $(2, 1, 2)$ in three dimensions.

and on Ω_{star} with $\hat{\mathbf{v}} = \hat{\mathbf{n}}$ and $\hat{\mathbf{v}} = \hat{\mathbf{r}}$, where $\hat{\mathbf{r}} = (x_1, x_2)/\sqrt{x_1^2 + x_2^2}$ is the radial vector. We see that in both cases, the condition number tends to ∞ as the string length $h \rightarrow 0$. Moreover, radially oriented strings outperform normally oriented strings for star-shaped domains. In either case, the condition number tends to improve as the string length increases. The oscillatory nature of the condition number for normally oriented strings is specific to the star-shaped domain owing to the oscillatory nature of the distance of the closest point to the boundary as h is increased. In both of the examples the same discretization was used for all h .

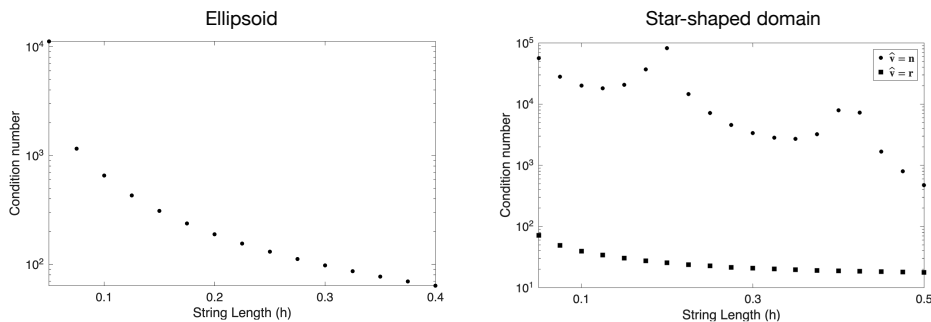


FIGURE 6. (Left) Condition number as a function of h for an ellipsoid with principal semi-axes $(2, 1, 2)$ in three dimensions, and (right) for the star-shaped domain Ω_{star} with $\hat{\mathbf{v}} = \hat{\mathbf{n}}$, and $\hat{\mathbf{v}} = \hat{\mathbf{r}}$.

Finally, to further illustrate the accuracy of the radial strings on star-shaped domains, we consider a “random” star-shaped domain whose parametrization is given by

$$\gamma_{\text{random}}(t) = \left(1 + 1.5 \sum_{i=1}^m (a_i \cos(it) + b_i \sin(it)) \right) \begin{bmatrix} \cos(t) \\ \sin(t) \end{bmatrix}, \quad t \in [0, 2\pi),$$

where a_i, b_i are i.i.d. standard Gaussians, and $m = 25$. Here $\hat{\mathbf{v}} = \hat{\mathbf{r}}$ with $h = 1.5$, $\lambda = 10$, and $\mu = 1$. Following an analogous procedure to that used in the prior examples, we generate an artificial solution using 200 random sources in the exterior and verify that the solution agrees with the exact solution up to a rigid body motion. The solution $u(\mathbf{x})$ and the pointwise residual $r(\mathbf{x})$ are plotted in Figure 7.

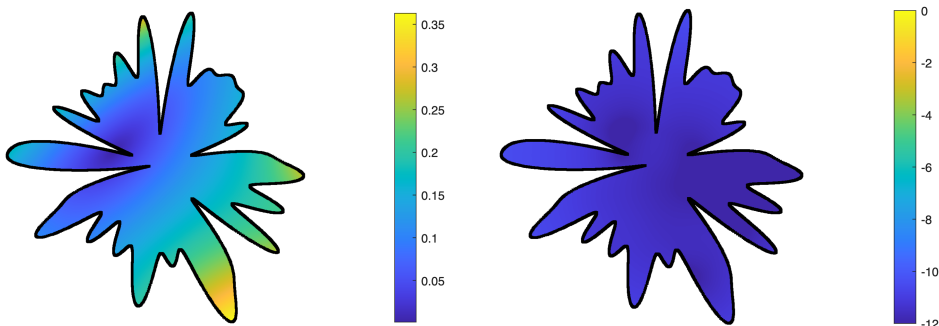


FIGURE 7. (left) computed solution $u(\mathbf{x})$ on Ω_{random} , and (right) \log_{10} of the relative residual $r(\mathbf{x})$.

6. CONCLUSION

In this work, we developed new string-based representations for the solution of traction boundary value problems in elastostatics. These representations adapt the Boussinesq-Cerruti solutions which are typically used for the construction of Green’s functions in half-spaces to generic exterior and interior boundary value problems. In particular, the singularity in the Boussinesq-Cerruti solutions extends along half-lines in the complementary domain, which we truncate, thereby enabling their use in non-convex domains in the interior and exterior problems.

The resulting integral equations on the boundary when using these ansatzes are second-kind Fredholm equations. These result in discretized linear systems whose condition number is independent of mesh size. This is illustrated in three dimensions by the constancy of the number of GMRES iterations as the mesh is refined. An additional advantage of integral equation methods is the absence of volumetric locking in the Stokes limit as $\lambda \rightarrow \infty$. The integral equation in two dimensions is independent of λ , and in three dimensions,

the condition number varies by less than a factor of 2 as λ is varied over thirteen orders of magnitude.

This string kernel approach can be immediately generalized to several other important applications, including time-harmonic elastodynamics, bi-harmonic and flexural wave problems [59, 4], acoustic boundary layers [51, 8], and generalized impedance boundary conditions [17]. In the above settings, existing integral representations tend to involve singular integral operators (which in many cases are preconditioned using the Hilbert transform to obtain a second-kind integral equation), or involve kernels requiring numerical inversion of Fourier transforms. String kernel representations provide an alternate approach for obtaining second-kind Fredholm equations for these problems, without operator composition. For scattering problems, string kernel type ansatzes can also be combined with coordinate complexification methods [24, 39, 31] to solve problems with infinite obstacles. All of these directions are being pursued and will be reported at a later date.

ACKNOWLEDGEMENTS

JGH was supported in part by a Sloan Research Fellowship. This research was supported in part by grants from the NSF (DMS-2235451) and Simons Foundation (MPS-NITMB-00005320) to the NSF-Simons National Institute for Theory and Mathematics in Biology (NITMB). AEL acknowledges support from the NSF under award DMS2052636. MR was supported in part by the Anusandhan National Research Foundation (ANRF/ARG/2025/011989/MS and ANRF/ARGM/2025/002421/MTR).

REFERENCES

- [1] H. ANDRÄ, *Integration of singular integrals for the galerkin-type boundary element method in 3d elasticity*, Computer methods in applied mechanics and engineering, 157 (1998), pp. 239–249.
- [2] D. N. ARNOLD, J. DOUGLAS JR, AND C. P. GUPTA, *A family of higher order mixed finite element methods for plane elasticity*, Numerische Mathematik, 45 (1984), pp. 1–22.
- [3] T. ASKHAM, Z. GIMBUTAS, L. GREENGARD, L. LU, J. MAGLAND, D. MALHOTRA, M. O’NEIL, M. RACHH, V. ROKHLIN, AND F. VICO, *fmm3d documentation: <https://github.com/flatironinstitute/fmm3d>*, GitHub Respository.
- [4] T. ASKHAM, T. GOODWILL, J. G. HOSKINS, P. NEKRASOV, AND M. RACHH, *Surface layers and linearized water waves: a boundary integral equation framework*, 2025.
- [5] T. ASKHAM, L. GREENGARD, J. G. HOSKINS, L. LU, M. O’NEIL, M. RACHH, F. VICO, AND V. ROKHLIN, *fmm3dbie*, 2025.
- [6] T. ASKHAM, M. RACHH, M. O’NEIL, J. G. HOSKINS, D. FORTUNATO, S. JIANG, F. FRYKLUND, T. GOODWILL, H. Y. WANG, AND H. ZHU, *chunkie: A MATLAB integral equation toolbox*, 2024.
- [7] I. BABUŠKA AND M. SURI, *Locking effects in the finite element approximation of elasticity problems*, Numerische Mathematik, 62 (1992), pp. 439–463.
- [8] M. BERGGREN, A. BERNLAND, AND D. NORELAND, *Acoustic boundary layers as boundary conditions*, Journal of Computational Physics, 371 (2018), pp. 633–650.
- [9] P. B. BOCHEV AND R. B. LEHOUCQ, *Energy principles and finite element methods for pure traction linear elasticity.*, Comput. Methods Appl. Math., 11 (2011), pp. 173–191.
- [10] D. BOFFI, F. BREZZI, AND M. FORTIN, *Mixed Finite Element Methods and Applications*, vol. 44 of Springer Series in Computational Mathematics, Springer, 2013.

- [11] M. BONNET, *Boundary Integral Equation Methods for Elastic and Plastic Problems*, John Wiley & Sons, Ltd, 2017, pp. 1–33.
- [12] J. BOUSSINESQ, *Application des potentiels à l'étude de l'équilibre et du mouvement des solides élastiques*, Gauthier-Villars, Paris, 1885. Digitized by Google from the library of the University of Michigan.
- [13] J. BREMER, Z. GIMBUTAS, AND V. ROKHLIN, *A nonlinear optimization procedure for generalized Gaussian quadratures*, SIAM J. Sci. Comput., 32 (2010), pp. 1761–1788.
- [14] S. BRENNER AND R. SCOTT, *The Mathematical Theory of Finite Element Methods*, Texts in Applied Mathematics, Springer New York, 2007.
- [15] S. C. BRENNER AND L.-Y. SUNG, *Linear finite element methods for planar linear elasticity*, mathematics of computation, 59 (1992), pp. 321–338.
- [16] A. BROMS, A. H. BARNETT, AND A.-K. TORNBERG, *Accurate close interactions of stokes spheres using lubrication-adapted image systems*, Journal of Computational Physics, 523 (2025), p. 113636.
- [17] F. CAKONI AND R. KRESS, *Integral equation methods for the inverse obstacle problem with generalized impedance boundary condition*, Inverse Problems, 29 (2012), p. 015005.
- [18] Y. CAO, W. W. SCHULTZ, AND R. F. BECK, *Three-dimensional desingularized boundary integral methods for potential problems*, International Journal for Numerical Methods in Fluids, 12 (1991), pp. 785–803.
- [19] V. CERRUTI, *Ricerche intorno all'equilibrio de' corpi elastici isotropi: memoria*, Salviucci, Roma, 1882.
- [20] S. CHRISTIANSEN, *On Kupradze's functional equations for plane harmonic problems*, Function theoretic methods in differential equations, (1976), pp. 205–243.
- [21] E. CORONA, L. GREENGARD, M. RACHH, AND S. VEERAPANENI, *An integral equation formulation for rigid bodies in stokes flow in three dimensions*, Journal of Computational Physics, 332 (2017), pp. 504–519.
- [22] E. CORONA, P.-G. MARTINSSON, AND D. ZORIN, *An $O(N)$ direct solver for integral equations on the plane*, Applied and Computational Harmonic Analysis, 38 (2015), pp. 284–317.
- [23] T. DUPONT, P. PERCELL, R. SCOTT, ET AL., *A family of finite elements with optimal approximation properties for various galerkin methods for 2nd and 4th order problems*, RAIRO. Analyse numérique, 13 (1979), pp. 227–255.
- [24] C. L. EPSTEIN, L. GREENGARD, J. G. HOSKINS, S. JIANG, AND M. RACHH, *Coordinate complexification for the helmholtz equation with dirichlet boundary conditions in a perturbed half-space*, 2025.
- [25] G. FAIRWEATHER AND A. KARAGEORGHIS, *The method of fundamental solutions for elliptic boundary value problems*, Advances in computational mathematics, 9 (1998), pp. 69–95.
- [26] R. S. FALK, *Nonconforming finite element methods for the equations of linear elasticity*, mathematics of computation, 57 (1991), pp. 529–550.
- [27] ———, *Finite element methods for linear elasticity*, in Mixed Finite Elements, Compatibility Conditions, and Applications: Lectures given at the CIME Summer School held in Cetraro, Italy June 26–July 1, 2006, Springer, 2008, pp. 159–194.
- [28] FMM2D, <https://github.com/flatironinstitute/fmm2d>, GitHub Respository.
- [29] Z. GIMBUTAS AND L. GREENGARD, *A fast multipole method for the evaluation of elastostatic fields in a half-space with zero normal stress*, Advances in Computational Mathematics, 42, pp. 175–198.
- [30] Z. GIMBUTAS, L. GREENGARD, M. BARALL, AND T. E. TULLIS, *On the calculation of displacement, stress, and strain induced by triangular dislocations*, Bulletin of the Seismological Society of America, 102 (2012), pp. 2776–2780.
- [31] T. GOODWILL, L. GREENGARD, J. G. HOSKINS, M. RACHH, AND Y. WANG, *Fast multipole method with complex coordinates*, 2025.
- [32] M. D. GRAHAM, *Microhydrodynamics, Brownian motion, and complex fluids*, vol. 58, Cambridge University Press, 2018.
- [33] L. GREENGARD, D. GUEYFFIER, P.-G. MARTINSSON, AND V. ROKHLIN, *Fast direct solvers for integral equations in complex three-dimensional domains*, Acta Numerica, 18 (2009), pp. 243–275.
- [34] L. GREENGARD, M. C. KROPINSKI, AND A. MAYO, *Integral equation methods for stokes flow and isotropic elasticity in the plane*, Journal of Computational Physics, 125 (1996), pp. 403–414.

- [35] L. GREENGARD, M. O'NEIL, M. RACHH, AND F. VICO, *Fast multipole methods for the evaluation of layer potentials with locally-corrected quadratures*, J. Comput. Phys.: X, 10 (2021), p. 100092.
- [36] L. GREENGARD AND V. ROKHLIN, *A fast algorithm for particle simulations*, J. Comput. Phys., 73 (1987), pp. 325–348.
- [37] J. HELSING, *On the interior stress problem for elastic bodies*, J. Appl. Mech., 67 (2000), pp. 658–662.
- [38] H.-K. HONG AND J.-T. CHEN, *Derivations of integral equations of elasticity*, Journal of Engineering Mechanics, 114 (1988), pp. 1028–1044.
- [39] J. G. HOSKINS, M. RACHH, AND B. WU, *On quadrature for singular integral operators with complex symmetric quadratic forms*, Applied and Computational Harmonic Analysis, 74 (2025), p. 101721.
- [40] G. C. HSIAO AND W. L. WENDLAND, *Boundary integral equations*, Springer, 2008.
- [41] M. A. JASWON, G. T. SYMM, AND T. CRUSE, *Integral equation methods in potential theory and elastostatics*, (1978).
- [42] R. P. KANWAL, *Integral equations formulation of classical elasticity*, Quarterly of Applied Mathematics, 27 (1969), pp. 57–65.
- [43] A. KARAEV AND E. STRELNIKOVA, *Singular integrals in axisymmetric problems of elastostatics*, International Journal of Modeling, Simulation, and Scientific Computing, 11 (2020), p. 2050003.
- [44] H. KERSTEN, *Grenz-und sprungrelationen für potenziale mit quadrat-summierbarer flächenbelegung*, Results in Mathematics, 3 (1980), pp. 17–24.
- [45] M. KESHAVARZI, *A modified integral equation applied to problems of elastostatics*, Computer Methods in Applied Mechanics and Engineering, 16 (1978), pp. 1–9.
- [46] S. KIM AND S. J. KARRILA, *Microhydrodynamics*, Butterworth-Heinemann, 1991.
- [47] R. KRESS, *Linear Integral Equations*, Springer, New York, NY, 2014.
- [48] V. KUPRADZE, *Potential methods in elasticity theory*, tech. rep., 1967.
- [49] L. LANDAU AND E. LIFSHITZ, *Theory of Elasticity*, A-W series in advanced physics, Pergamon Press, 1959.
- [50] G. LAURICELLA, *Sur l'intégration de l'équation relative à l'équilibre des plaques élastiques écastrées*, Acta mathematica, (1909), pp. 201–256.
- [51] J. LINDEN, T. ASKHAM, AND J. G. HOSKINS, *A boundary integral formulation of an acoustic boundary layer model in 2d*, 2026.
- [52] A. LOVE, *A Treatise on the Mathematical Theory of Elasticity*, Cambridge University Press, 2013.
- [53] J. MA, V. ROKHLIN, AND S. WANDZURA, *Generalized Gaussian quadrature rules for systems of arbitrary functions*, SIAM J. Numer. Anal., 33 (1996), pp. 971–996.
- [54] P.-G. MARTINSSON AND V. ROKHLIN, *A fast direct solver for boundary integral equations in two dimensions*, Journal of Computational Physics, 205 (2005), pp. 1–23.
- [55] S. G. MIKHLIN, *Integral equations: and their applications to certain problems in mechanics, mathematical physics and technology*, vol. 4, Elsevier, 2014.
- [56] V. MINDEN, K. L. HO, A. DAMLE, AND L. YING, *A recursive skeletonization factorization based on strong admissibility*, Multiscale Modeling & Simulation, 15 (2017), pp. 768–796.
- [57] R. MINDLIN, *Force at a point in the interior of a semi-infinite solid*, Physics, 7 (1936), p. 195–202.
- [58] N. I. MUSKHELISHVILI ET AL., *Some basic problems of the mathematical theory of elasticity*, vol. 15, Noordhoff Groningen, 1953.
- [59] P. NEKRASOV, Z. SU, T. ASKHAM, AND J. G. HOSKINS, *Boundary integral formulations for flexural wave scattering in thin plates*, Journal of Computational Physics, 542 (2025), p. 114355.
- [60] V. PARTON AND P. PERLIN, *Integral equation methods in elasticity*, MIR, Moscow, (1982).
- [61] C. POZRIKIDIS, *Boundary integral and singularity methods for linearized viscous flow*, Cambridge university press, 1992.
- [62] J. PUNCHIN, *Weakly singular integral operators as mappings between function spaces*, The Journal of Integral Equations and Applications, (1988), pp. 303–320.
- [63] M. RACHH AND L. GREENGARD, *Integral equation methods for elastance and mobility problems in two dimensions*, SIAM J. Numer. Anal., 54 (2016), pp. 2889–2909.

- [64] J. SCHUR, *Bemerkungen zur theorie der beschränkten bilinearformen mit unendlich vielen veränderlichen.*, (1911).
- [65] C. SCHWAB AND W. L. WENDLAND, *On numerical cubatures of singular surface integrals in boundary element methods*, *Numerische Mathematik*, 62 (1992), pp. 343–369.
- [66] D. I. SHERMAN, *Solution to plane elastic problems with given outside forces*, *Dokl. Akad. Nauk. SSSR*, 28 (1940), pp. 25–28.
- [67] D. SUSHNIKOVA, L. GREENGARD, M. O’NEIL, AND M. RACHH, *FMM-LU: A fast direct solver for multiscale boundary integral equations in three dimensions*, *Multiscale Model. Simul.*, 21 (2023), pp. 1570–1601.
- [68] A.-K. TORNBORG AND L. GREENGARD, *A fast multipole method for the three-dimensional stokes equations*, *Journal of Computational Physics*, 227 (2008), pp. 1613–1619.
- [69] B. VIOREANU AND V. ROKHLIN, *Spectra of Multiplication Operators as a Numerical Tool*, *SIAM J. Sci. Comput.*, 36 (2014), pp. A267–A288.
- [70] S. VOGEL AND F. RIZZO, *An integral equation formulation of three dimensional anisotropic elastostatic boundary value problems*, *Journal of Elasticity*, 3 (1973), pp. 203–216.
- [71] H. XIAO AND Z. GIMBUTAS, *A numerical algorithm for the construction of efficient quadrature rules in two and higher dimensions*, *Computers & mathematics with applications*, 59 (2010), pp. 663–676.
- [72] J. YAO, B. XIE, AND J. LAI, *A robust and high precision algorithm for elastic scattering problems from cornered domains*, *Journal of Scientific Computing*, 98 (2024), p. 65.
- [73] N. YARVIN AND V. ROKHLIN, *Generalized Gaussian quadratures and singular value decompositions of integral operators*, *SIAM J. Sci. Comput.*, 20 (1998), pp. 699–718.
- [74] O. C. ZIENKIEWICZ AND R. L. TAYLOR, *The finite element method for solid and structural mechanics*, Elsevier, 2005.